Maximal entangling rates from holography

Åsmund Folkestad
Center for Theoretical Physics, Massachusetts Institute of Technology, Cambridge, Massachusetts 02139, USA and Kavli Institute for Theoretical Physics, University of California, Santa Barbara, California 93106, USA

Aditya Dhumuntarao
School of Physics and Astronomy, University of Minnesota, Minneapolis, Minnesota 55455, USA and Martin A. Fisher School of Physics, Brandeis University, Waltham, Massachusetts 02453, USA

(Received 3 July 2023; accepted 4 October 2023; published 30 October 2023)

We prove novel far-from-equilibrum bounds on conformal field theories, upper bounding the growth rate of entanglement entropy in spatially uniform states. When equal-time correlators and Wilson loops are computed by geodesics and world sheets, we also bound the growth rate of these. Example applications include lower bounds on thermalization times or the time it takes to achieve deconfinement. Our bounds are proven for holographic conformal field theories at strong coupling and large–N, but we provide evidence that they are valid independent of these assumptions. In two dimensions, our results prove a conjectured bound on entanglement growth by Liu and Suh for a large class of states. We also derive bounds on spatial derivatives of correlation measures. From a gravitational perspective, our results constitute new lower bounds on the mass of asymptotically AdS spacetimes with planar symmetry, strengthening the positive mass theorem for these spacetimes. We also derive novel relations in AdS/CFT relating various geometric features directly to entanglement entropy derivatives. For example, we show that conformal field theory entanglement growth corresponds to bulk matter falling deeper into the bulk.

DOI: 10.1103/PhysRevD.108.086032

I. INTRODUCTION

Entanglement is one of the defining features of quantum mechanics, and its effects are ubiquitous in modern physics. It is now understood that entanglement entropy plays a significant role in a variety of fields, including quantum many-body physics [1–3], quantum information theory [4–6], quantum gravity [7–21], and renormalization group flows in quantum field theory [22–30].

A central question relevant to the above subjects is how entanglement behaves dynamically. In this paper, we address the following question: can we find growth bounds on the entanglement entropy and other correlation measures, even when we are far from equilibrium or when the coupling is strong? Answering these questions is relevant to understanding how rapidly quantum information can propagate, how long it takes a many-body system to thermalize, bounding decoherence times, or, in quantum gravity, for constraining the dynamics of emergent spacetime.

Published by the American Physical Society under the terms of the Creative Commons Attribution 4.0 International license. Further distribution of this work must maintain attribution to the author(s) and the published article's title, journal citation, and DOI. Funded by SCOAP³.

While calculating entanglement entropies is notoriously hard, several lessons have nevertheless been learned over the last two decades. Quantum quenches in particular have been a fruitful arena of inquiry. In a quantum quench, the Hamiltonian is abruptly changed, or a source is turned on over a small time interval δt. In either case, there is an abrupt injection of energy into the system, kicking an initially stationary state out of equilibrium. The subsequent approach to equilibrium can then be computed in various setups. For example, in a seminal paper by Calabrese and Cardy [23], the entanglement entropy S_R of an interval R of length ℓ in a $(1+1)$-dimensional conformal field theory (CFT) after a uniform quench was computed. For large times and interval lengths, it was found to behave as

$$S_R(t) - S_R(t=0) = \begin{cases} 2s_{\mathrm{th}}t & t < \ell/2 \\ s_{\mathrm{th}}\ell & t \geq \ell/2 \end{cases}, \qquad (1)$$

where s_{th} the thermal entropy density of the final state. Linear growth of entanglement for large regions R after uniform quenches has also been found in higher dimensional holographic CFTs [31–34]. In particular, after local equilibration and before late time saturation, the entanglement entropy of a region R after a quench was found to behave as [33,34]

$$S_R(t) - S_R(t=0) = v_E s_{\text{th}} \text{Area}[\partial R] t + \ldots \tag{2}$$

with v_E the so-called entanglement velocity, which satisfies $v_E \leq 1$.

Quenches provide rich insights on entanglement dynamics, and they have inspired powerful phenomenological models for entanglement dynamics that reproduce findings of quenches [35–37]. However, quenches represent special setups, and it would be useful to understand whether lessons learned from quenches represent the much larger space of possible far-from-equilibrium states. Some results covering more general states do exist. Consider two quantum systems $A \cup a$ and $B \cup b$ coupled by an interaction Hamiltonian H_{AB} acting only on the subsystems A and B. In [38] (building on [39]) it was proven that

$$\left| \frac{\mathrm{d}S_{A\cup a}}{\mathrm{d}t} \right| \leq \eta \|H_{AB}\| \log d, \tag{3}$$

where $d = \min\{\dim A, \dim B\}$, and where η is an order 1 constant. While this bound has broad generality for finite-dimensional systems, it is not useful in QFT, where d is infinite. Even if we UV-regulate to make d finite, the norm of the interaction Hamiltonian is infeasible to compute. Furthermore, the bound is state-independent, and it is natural to suspect the rate of entanglement growth under Hamiltonian evolution is limited by the energy of the system. Thus, in local quantum many-body systems with conservation of energy, we would expect that more powerful bounds exist.

A bound on entanglement growth useful in QFT was conjectured in [33,34], based on the findings in holographic quenches. It was proposed that a normalized instantaneous entanglement growth $\mathfrak{R}$ in relativistic QFT satisfies the bound

$$\mathfrak{R} \equiv \frac{1}{\text{Area}[\partial R] s_{\text{th}}} \left| \frac{\mathrm{d}S_R}{\mathrm{d}t} \right| \leq 1. \tag{4}$$

The authors of [40] utilized relativistic QFT to prove that, for convex regions R in spatially uniform states, $\mathfrak{R} \leq 1$ holds to leading order in a large subregion expansion, where nonextensive contributions to S_R were neglected [41]. However, it was found in [34] that the largest values for $\mathfrak{R}$ were obtained for intermediate sized regions, where existing proofs of $\mathfrak{R} \leq 1$ do not apply. Thus, the validity of (4) for general regions is still an open question [44].

In this work, we will prove novel speed limits on the growth of entanglement, and in some cases other correlation measures, in a large class of CFTs far-from-equilibrium. Our bounds will imply $\mathfrak{R} \leq 1$ for a number of situations not previously covered—in particular, our results are not restricted to quenches or large subregions. We will however need to make some restrictions. First, we will work with spatially uniform states. Next, we will work with holographic CFTs at strong coupling and large N (large effective number of degrees of freedom), so that we can utilize the equivalent dual gravitational description available through the AdS/CFT correspondence. For several of our bounds, however, we will provide evidence that they are valid for CFTs more broadly, even when they are not holographic, strongly coupled, or at large–N. Finally, for technical reasons we will have to assume that certain scalar single trace operators have vanishing one-point functions, but we will again provide evidence that our bounds are true irrespective of these assumptions, even though we cannot give a proof.

Let us now summarize our results. We start with 2d, where our results are strongest. Consider a 2d CFT on Minkowski space in a homogeneous and isotropic state undergoing time-evolution. Let t label the time slices on which the state is uniform, and let R be a union of intervals of any size. Assuming an energy condition and certain falloff conditions on the matter fields in the bulk, whose CFT interpretation we will discuss below, we prove that

$$\left| \frac{\mathrm{d}S_R}{\mathrm{d}t} \right| \leq n \sqrt{\frac{8\pi c}{3} \langle T_{tt} \rangle}, \tag{5}$$

where c is the central charge and $\langle T_{tt} \rangle$ the CFT energy density one-point function, which is the same everywhere in a uniform state. This is our main result. If we work with uncharged states, (5) implies that $\mathfrak{R} \leq 1$. Thus, for the $2d$ theories under consideration, we have given a proof of $\mathfrak{R} \leq 1$ to regions of arbitrary finite size and with any number of connected components [46].

Next, in cases where the geodesic approximation can be utilized, we prove that

$$\left| \frac{\mathrm{d}}{\mathrm{d}t} \log \langle O(x) O(0) \rangle_{\rho(t)} \right| \leq \sqrt{\frac{96\pi \Delta^2}{c} \langle T_{tt} \rangle}, \tag{6}$$

where $O(x)$ is a heavy primary operator of scaling dimension $\Delta \gg 1$. This bound is respected (and in certain regimes saturated) in the global CFT_2 quenches studied in [47,48] (even when Δ and c are not large). The fact that (5) and (6) are saturated in direct CFT computations that make no assumption of holography, large central charge or strong coupling suggest that these bounds could be true beyond the context in which we have proven them.

Next, for small separations x, we prove a stronger bound on heavy correlators, again valid in the cases where geodesic approximation holds:

$$\left| \frac{\mathrm{d}}{\mathrm{d}t} \log \langle O(x) O(0) \rangle_{\rho(t)} \right| \leq \frac{12\pi \Delta |x|}{c} \langle T_{tt} \rangle [1 + \ldots], \tag{7}$$

where dots indicate $\mathcal{O}(x^2 \langle T_{tt} \rangle / c)$ corrections. Before turning to higher dimensions, we note that the bounds (5)–(7)

are valid also for CFTs on a spatial circle, provided we replace $\langle T_{tt}\rangle \to \langle T_{tt}\rangle - \langle T_{tt}\rangle_{\text{vacuum}}$.

Next, consider $d \geq 2$-dimensional holographic CFTs on Minkowski space, again in a time-evolving uniform state. Taking R to be either a single ball or strip of characteristic size ℓ, we prove that

$$\left|\frac{\mathrm{d}S_R}{\mathrm{d}t}\right| \leq \kappa \mathrm{Vol}[R]\langle T_{tt}\rangle\left[1+\mathcal{O}\left(\frac{\ell^d\langle T_{tt}\rangle}{c_{\text{eff}}}\right)\right], \qquad (8)$$

where κ is an $O(1)$ numerical constant given in the main text [see (29)], and which depends only on d and the shape of R. c_{eff} is the effective central charge, which for a given theory can be extracted from the vacuum entanglement entropy—see main text. This bound is only applicable for small regions, but it is much stronger than $\mathfrak{R} \leq 1$ [49]. For an uncharged state, if β is the effective inverse temperature at which the thermal energy density equals $\langle T_{tt}\rangle$, we have shown that $\mathfrak{R} \leq \mathcal{O}(\ell^d/\beta^d) \ll 1$.

We also prove a higher-dimensional analog of (5), although in this case the proof is more limited. Consider a family of states where in the gravitational description, all nongauge-field matter is localized to a thin planar shell, which under the radius-scale duality in AdS/CFT corresponds to states where all dynamics at a given time takes place at a single (time-dependent) energy scale. For these states we prove that

$$\left|\frac{\mathrm{d}S_R}{\mathrm{d}t}\right| \leq \frac{1}{4}\mathrm{Area}[\partial R]c_{\text{eff}}\left[\frac{16\pi}{(d-1)c_{\text{eff}}}\langle T_{tt}\rangle\right]^{\frac{d-1}{d}}, \qquad (9)$$

where R either is a single ball or the union of any number of strips. Considering a neutral state whose holographic dual is a uncharged black brane, (9) translates into $\mathfrak{R} \leq 1$. While our proof of (9) applies to a smaller class of states, we give substantial numerical evidence that it holds more generally for all uniform states—at least in holographic CFTs.

Next, for the special case of $d = 4$, we prove bounds on Wilson loops $\mathcal{W}(C)$ of spacelike circles C, assuming we can compute these using classical worldsheets in the gravitational bulk. Like for the geodesic approximation, we do not claim that this approximation is always valid (see for example [51]). However, when it is justified to use it, we do get a bound. In terms of the variables characterizing $\mathcal{N} = 4$ super Yang-Mills with the gauge group $SU(N)$ and 't Hooft coupling λ, we then show that

$$\left|\frac{\mathrm{d}}{\mathrm{d}t}\log\langle\mathcal{W}(C)\rangle_{\rho(t)}\right| \leq \mathrm{Length}[C]\sqrt{\frac{2\lambda}{3N^2}\langle T_{tt}\rangle}. \qquad (10)$$

For other potential $d = 4$ holographic CFTs, our result can be written in terms of the effective central charge and effective coupling—see main text. In $d = 3$, we prove a similar result, but for the more restricted set of states where all dynamics is restricted to a single energy scale [see (134)]. For small Wilson loops, we again have stricter bounds, which we give in the main text [see (130)]. If we have a phase transition with onset of confinement, bounds of the form (10) could be used to bound how rapidly Wilson loops can transition from a phase perimeter law to a phase with area law.

Let us now comment on the energy condition and asymptotic falloffs at large radius assumed in the gravitational bulk for the proofs. We assume the dominant energy condition, which in the CFT most significantly implies that the one-point functions of relevant scalar primary operators ($\Delta < d$) should be vanishing in our states. However, we provide strong numerical evidence, and some more general arguments, that the dominant energy condition is unnecessary, although we cannot prove it. Next, the falloff condition precisely corresponds to the assumption that one-point functions for relevant scalar primary operators with scaling dimension in the restricted band $\frac{d-2}{2} \leq \Delta < \frac{d}{2}$ are vanishing. However, since the proofs of $\mathfrak{R} \leq 1$ for large connected convex subregions do not require the absence of such operators, nor does the Calabrese-Cardy global quench computation that respects our bounds, it is plausible that our bounds are true also in states violating this assumption.

Let us now sketch the broad picture of how our bounds are proven, restricting to the time-derivative of the entanglement entropy of a strip for concreteness. For CFTs dual to classical Einstein gravity, the von Neumann entropy of the reduced state ρ_R on a subregion R is given by the HRT formula [10,11,52], which says that

$$S_R = \frac{\mathrm{Area}[X]}{4G_N}, \qquad (11)$$

where X is the so-called HRT surface in the gravitational dual spacetime, which roughly means a codimension 2 spacelike surface that has stationary area under compact perturbations of X. Bounding $\partial_t S_R$ in uniform states now corresponds to bounding $\partial_t \mathrm{Area}[X_t]$, where X_t is a one-parameter family of surfaces living in general time-dependent spacetimes with planar symmetry. Central to our proof is showing that the change in entanglement entropy is given by

$$\frac{\mathrm{d}S_R}{\mathrm{d}t} = \int_{X_t} GP, \qquad (12)$$

where P is the matter momentum density in a direction orthogonal to HRT surface, and where G essentially is a propagator that only depends on the smallest radius probed by X_t, and not any other details of the spacetime. We thus see that the flux of matter falling across the HRT surface is directly responsible for the increase in entanglement entropy. The formula (12) can be seen as a new momentum-entanglement correspondence in AdS/CFT, analog to the momentum-complexity correspondence proposed by Susskind in [53] and given a precise form in [54–56].

To leverage (12) to get our proofs, we study two quasilocal masses and that find that in certain dimensions, the integral in (12) is exactly encoded in the difference between these two quasilocal masses at infinity. This follows from an analysis of the monotonicity properties of these masses, essentially through a combination of so-called Lorentzian and Riemannian inverse mean curvature flows. To our knowledge, our proof techniques leveraging this delicate interplay between these two quasilocal masses is novel, and the power of our methods our highlighted by that fact that our bounds alternatively can be viewed as lower bounds on $\langle T_{tt}\rangle$, i.e. strengthenings of the positive mass theorem.

In constructing our proofs, we also prove several new relationships between geometry and CFT entanglement in AdS/CFT. In addition to the relation between $\partial_t S$ and the infalling matter momentum, we prove that for strip-shaped region R (or an interval for 2d), we have

$$\partial_x S_R = \frac{\mathrm{Area}[\partial R]}{4G_N}\left(\frac{r_0}{L}\right)^{d-1}, \tag{13}$$

where G_N is Newton's constant, r_0 is the smallest radius probed by the HRT surface, and L the AdS radius, which is simply related to the cosmological constant. That is, for uniform states, the derivative with respect to strip width is exactly determined by how deep into the bulk spacetime the surface probes. From this, we for example see that $\partial_x^2 S \to 0$ geometrically means that the HRT surface on the gravity side is encountering a barrier, preventing it from reaching deeper into the spacetime. This suggests the presence of a horizon.

This paper is organized as follows. In Sec. II we set up our assumptions and prove our entanglement growth bounds for when the subregion R is a strip. We also prove our correlator bounds for $d = 2$ in this section. In Sec. III we prove the entanglement growth bounds for ball shaped regions R and furthermore derive general properties $(q+1)$-dimensional extremal surfaces anchored at q-dimensional spheres on the boundary, leading to our results for Wilson loops and a new general class of lower bounds on the spacetime mass in odd-dimensional spacetimes. In Sec. IV we prove bounds on spatial derivatives of the entanglement entropy of strips in general dimensions and equal-time two-point correlators in $d = 2$. In Sec. V, for a subset of our bounds, we give numerical evidence that the dominant energy condition is not required. Finally, in Sec. VI, we conclude with a discussion of the implications of our findings, together with future directions. For a reader only wanting to understand the results without getting into the details of the proofs, it is possible to only read Secs. II A, III A, and IV–VI.

II. BOUNDS FOR STRIPS AND CORRELATORS

A. Setup and summary of results

Consider a d-dimensional holographic CFT in Minkowski space dual to classical Einstein gravity, so that we are working to leading order in large N. Consider now some general time-evolving state $\rho(t)$ possessing a geometric dual, and having spatially homogeneous and isotropic one-point functions for local operators dual to bulk fields, such as the CFT stress tensor T_{ij}. Homogeneity and isotropy ensures that the dual asymptotically AdS$_{d+1}$ spacetime $(\mathcal{M}, g)$ has planar symmetry. We allow $\rho(t)$ to live on either one or two copies of Minkowski space, so that the dual spacetime can have either one or two asymptotic boundaries. For a single system, we allow $\rho(t)$ to be mixed [57].

Our goal in this section is to use the HRT entropy formula in this setup to derive a speed limit on the growth of the entanglement for a strip, and in some cases the union of any number of strips, provided they all live on the same connected component of the conformal boundary. Since HRT surfaces in two dimensions are geodesics, our results for entanglement entropy will also imply bounds on correlators computed by geodesics. In Sec. III we will generalize to spherical subregions, and to Wilson loops. However, we will present the results on entanglement growth for spherical regions in this section, since they naturally are presented together with the results for strips.

Before presenting our results, let us set up our assumptions. We will assume that our spacetimes are AdS-hyperbolic, meaning that we can foliate $(\mathcal{M}, g_{ab})$ with spacelike hypersurfaces Σ_t that all have the same topology and are geodesically complete as Riemannian manifolds. These represent moments of time. Next, letting L be the asymptotic AdS radius, we assume that $(\mathcal{M}, g_{ab})$ satisfies the Einstein equations

$$R_{ab} - \frac{1}{2}g_{ab}R - \frac{d(d-1)}{2L^2}g_{ab} = 8\pi G_N \mathcal{T}_{ab}, \tag{14}$$

and that the dominant energy condition (DEC) holds for the bulk stress tensor $\mathcal{T}_{ab}$, meaning that

$$\mathcal{T}_{ab}u^a v^b \geq 0 \quad \text{for all timelike } u^a, v^b. \tag{15}$$

Next, we assume that the matter fields fall off sufficiently fast at infinity so that the Balasubramanian-Kraus [59] boundary stress tensor $\langle T_{ij}\rangle$ is finite. When it is finite, it corresponds to the one-point function of the CFT stress tensor. To specify falloff assumptions more explicitly, let Ω be any defining function, meaning any function on the conformal compactification of $\mathcal{M}$ such that the pullback of $\Omega^2 g_{ab}|_{\partial\mathcal{M}}$ to the conformal boundary is a Lorentzian metric. We then require that the bulk stress tensor satisfies

$$\mathcal{T}_{ab}u^a v^b \sim o(\Omega^d), \quad \forall \text{ unit vectors } v^a, u^a, \tag{16}$$

near the conformal boundary $\partial\mathcal{M}$. In the radial coordinate r introduced below, this means the stress tensor in an orthonormal basis falls off as $o(r^{-d})$. Matter fields with falloffs sufficiently slow to require modifications of the definition of the spacetime mass are not covered by our results [60]. To avoid having to repeat the same assumptions in every theorem, let us define the following:

Definition 1. We say that an AAdS_{d+1} spacetime $(\mathcal{M}, g_{ab})$ is regular if it is AdS-hyperbolic, has falloffs (16), and g_{ab} is C^2.

For index conventions, we will take $a, b, \ldots$ to be abstract spacetime indices, and $\alpha, \beta, \ldots$ to be abstract indices on spacelike hypersurfaces Σ. We take $\mu, \nu, \ldots$ to be coordinate indices on Σ. Other indices should be clear in the context. Furthermore, whenever intrinsic tensors on submanifolds are written with spacetime indices, we mean the pushforward/pullback to spacetime using the embedding map.

To describe the boundary regions R covered by our results, we select a Minkowski conformal frame on the conformal boundary with coordinates

$$\mathrm{d}s^2|_{\partial\mathcal{M}} = -\mathrm{d}t^2 + L^2(\mathrm{d}\phi^2 + \mathrm{d}\boldsymbol{x}^2), \qquad (\phi, \boldsymbol{x}) \in \mathbb{R}^{d-1}, \tag{17}$$

where the constant t-slices are the ones on which we have uniform one-point functions for local operators. For $d = 2$ we can allow ϕ to be periodically identified, in which case we say that $\mathcal{M}$ has spherical symmetry. Now, if the conformal boundary $\partial\mathcal{M}$ has two connected components, we focus on a particular one. We then define $R_{t'}$ to be the one-parameter family of boundary regions given by

$$-\frac{\ell}{2L} \leq \phi \leq \frac{\ell}{2L}, \qquad t = t', \tag{18}$$

which just corresponds to a strip or interval of length ℓ at time t'. In this section, when we talk about strips or refer to a one-parameter family, we always mean the family (18). We will abbreviate $R_{t=0} \equiv R$, and define

$$\mathrm{Area}[\partial R_t] = \mathrm{Area}[\partial R] = L^{d-2} \int_{\mathbb{R}^{d-2}} \mathrm{d}^{d-2}\boldsymbol{x}, \quad d > 2, \tag{19}$$

while for $d = 2$, we have $\mathrm{Area}[\partial R] = 2$. For $d > 2$ this is of course divergent, but since it always appears as an overall prefactor it causes no difficulties.

Next, the HRT formula [10,11,52] states that the von Neumann entropy of the reduced CFT state on R_t, $\rho_R(t) \equiv \mathrm{tr}_{R^c}\rho(t)$, is given by

$$S_R(t) = -\mathrm{tr}[\rho_R(t) \ln \rho_R(t)] = \frac{\mathrm{Area}[X_t]}{4G_N}, \tag{20}$$

where X_t is the minimal codimension-2 spacelike surface in $(\mathcal{M}, g_{ab})$ that is (1) a stationary point of the area functional (i.e. extremal), (2) anchored at ∂R_t on the conformal boundary ($\partial X_t = \partial R_t$), and (3) homologous to R_t. The latter means that there exists spacelike hypersurface Σ with $\partial\Sigma = X_t \cup R_t$, where we here mean the boundary in the conformal completion. We will use the gravitational description to derive an upper bound on

$$\left| \frac{\mathrm{d}}{\mathrm{d}t} \left(\frac{\mathrm{Area}[X_t]}{4G_N} \right) \right| \tag{21}$$

purely in terms of quantities that have a known interpretation in the CFT. While $\mathrm{Area}[X_t]$ is formally divergent, since we (1) work with spacetimes with falloffs (16) and (2) $\mathrm{Area}[\partial R_t]$ is time-independent, (21) is in fact finite up to the constant $\mathrm{Area}[\partial R]$ prefactor.

Let us now summarize our main results, which are broadly divided into two categories. The first class of bounds scales like $\mathrm{Area}[\partial R]$, and they are strongest when R is large. The second class of bounds scales like $\mathrm{Vol}[R]$, and they are consequently the strongest for small subregions. For intermediate sized regions, where the entanglement entropy is about the enter the volume-scaling regime, we expect the two types of upper bounds to be roughly comparable.

First, for a three-dimensional bulk, we obtain the following

Theorem 1. Let $(\mathcal{M}, g_{ab})$ be a regular asymptotically AdS_3 spacetime with planar or spherical symmetry satisfying the DEC. Assume that X_t is the HRT surface of a finite interval R_t. Then

$$\left| \frac{\mathrm{d}}{\mathrm{d}t} \left(\frac{\mathrm{Area}[X_t]}{4G_N} \right) \right| \leq \sqrt{\frac{8\pi c}{3} (\langle T_{tt} \rangle - \langle T_{tt} \rangle_{\mathrm{vac}})}, \tag{22}$$

where $c = \frac{3L}{2G_N}$.

Since the HRT surface of a union of strips is just the union of HRT surfaces of a collection of individual strips, this bound immediately implies that if R is a union of n intervals contained in a single moment of time on one of the connected components of $\partial\mathcal{M}$, then

$$\left| \frac{\mathrm{d}}{\mathrm{d}t} S_R \right| \leq n \sqrt{\frac{8\pi c}{3} (\langle T_{tt} \rangle - \langle T_{tt} \rangle_{\mathrm{vac}})}. \tag{23}$$

While we are not able to give a general proof of the analog of Theorem 1 in higher dimensions, we prove a version in thin-shell spacetimes:

Theorem 2. Let $(\mathcal{M}, g_{ab})$ be an asymptotically $\mathrm{AdS}_{d+1\geq 3}$ spacetime with planar symmetry satisfying the DEC. Assume that X_t is the HRT surface of a region R_t corresponding to either a strip or a ball. Assume that the bulk matter consists of $U(1)$ gauge fields and a thin shell of matter:

$$\mathcal{T}_{ab} = \mathcal{T}_{ab}^{\text{shell}} + \mathcal{T}_{ab}^{\text{Maxwell}}, \tag{24}$$

where $\mathcal{T}_{ab}^{\text{shell}}$ has delta function support on a codimension–1 world volume that is timelike or null, and with $\mathcal{T}_{ab}^{\text{shell}}$ separately satisfying the DEC. Assume $(\mathcal{M}, g_{ab})$ is regular, except we do not require g_{ab} to be C^2 at the shell. Then

$$\left|\frac{\mathrm{d}}{\mathrm{d}t}\left(\frac{\text{Area}[X_t]}{4G_N}\right)\right| \leq \frac{1}{4}\text{Area}[\partial R]c_{\text{eff}}\left[\frac{16\pi}{(d-1)c_{\text{eff}}}\langle T_{tt}\rangle\right]^{\frac{d-1}{d}}, \tag{25}$$

where

$$c_{\text{eff}} = \frac{L^{d-1}}{G_N}. \tag{26}$$

As a special case, this theorem applies to thin-shell Vaidya spacetimes and charged generalizations. These spacetimes (and related setups) have been studied extensively [31–34,37,43,50,61–101] as holographic models CFT quenches. However, more general cases than Vaidya are allowed, where the shell might correspond to some energy-shell in the bulk interior, propagating in a timelike direction and never actually hitting the boundary. Using the duality between radius and scale in the CFT, thin shell spacetimes correspond to CFT states where all dynamics is happening at a single scale that evolves with time.

We also should note that (25) holds if R is a union of any number of strips on the same conformal boundary, due to the fact that the HRT surface of n strips is just equal to n HRT surfaces of n (generally different) strips. One can hope that this might also be true for multiple spheres or other shapes, but this does not follow from our proofs. Also, while we do not have a proof, we conjecture that (25) is valid in all DEC respecting regular planar symmetric AAdS_{d+1} spacetimes, and we provide strong numerical evidence for this in Sec. V. In fact, our numerics seem to indicate that the DEC is even unnecessary, as long as our theory has a stable AdS vacuum, which is required for a holographic dual CFT to have a Hamiltonian that is bounded below.

Also, note that c_{eff} can be defined purely in CFT in terms of a universal prefactor of the sphere vacuum entanglement entropy [10,52], or in terms of the renormalized entanglement entropy [102,103]. So our final bounds on $|\partial_t S|$ make no reference to the bulk.

The previous two theorems give upper bounds scaling like $\text{Area}[\partial R]$. Now let us turn to bounds scaling like $\text{Vol}[R]$. We prove the following bound on small regions, valid for all $d \geq 2$:

Theorem 3. Let $(\mathcal{M}, g_{ab})$ be a regular asymptotically $\text{AdS}_{d+1\geq 3}$ spacetime with planar symmetry satisfying the DEC. Assume that X_t is the HRT surface of a region R_t corresponding to either a strip or a ball. Let ℓ be either the strip width or ball radius, and assume that

$$\frac{\ell^d\langle T_{tt}\rangle}{c_{\text{eff}}} \ll 1. \tag{27}$$

Then

$$\left|\frac{\mathrm{d}}{\mathrm{d}t}\left(\frac{\text{Area}[X_t]}{4G_N}\right)\right| \leq \kappa_d \text{Vol}[R]\langle T_{tt}\rangle\left[1 + \mathcal{O}\left(\frac{\langle T_{tt}\rangle\ell^d}{c_{\text{eff}}}\right)\right], \tag{28}$$

where

$$\kappa_d = \frac{\Gamma\left(\frac{1}{2(d-1)}\right)}{\Gamma\left(\frac{d}{2(d-1)}\right)}\begin{cases} 2\pi & R \text{ is an interval and } d = 2, \\ \frac{\sqrt{\pi}}{d-1} & R \text{ is a strip and } d > 2, \\ 2\sqrt{\pi} & R \text{ is a ball and } d > 2. \end{cases} \tag{29}$$

For thin shell spacetimes, volume-type bounds like the one above can be proven exactly for subregions of any size, at the cost of a slightly larger prefactor. See Theorem 5.

We will now outline the strategy used to obtain these bounds. First, we show that there exists exactly one homology hypersurface Σ_t that both contains X_t, and which respects the planar symmetry of $(\mathcal{M}, g_{ab})$. Then we show that the location of X_t on Σ_t can be solved for exactly in terms of the intrinsic geometry on Σ_t. Together with the DEC, this fact allows us to lower bound the radius of the tip of the HRT surface. Next, we use the fact that since X_t is extremal, the first order variation of its area is a pure boundary term located at ∂X_t [104], and we show that this boundary term is simply given by a particular component of the extrinsic curvature of Σ_t as $r \to \infty$. Then we work out the form of Einstein constraint equations on Σ_t, and show that the relevant extrinsic curvature component can be written as an integral of the matter flux over the HRT surface. Finally, essentially relying on inverse mean curvature flow of Lorentzian and Riemannian Hawking masses, and their monotonicity properties under these flows, we bound the integrated matter flux across the HRT surface from above in terms of the mass of the spacetime.

Now, before we dive in, we should clarify the meaning of radii in planar symmetric spacetimes. Since we have planar symmetry, spacetime has a two-parameter foliation where each leaf is a codimension–2 spacelike plane that has the usual flat intrinsic metric. When we talk about a plane, we always mean one of these leafs. These planes can all be assigned an "area radius" r, and it is possible to view r as a scalar function on spacetime which is not tied to any coordinate. Nevertheless, unlike in spherical symmetry, there is an overall scaling ambiguity in this function, since the noncompactness of the planes means we cannot normalize r to some area—there is no "unit plane." However, if we choose some Minkowski conformal frame on the boundary, we can fix the overall normalization of r by demanding that the defining function Ω that takes us to the chosen conformal frame is $\Omega = r/L$. We will implicitly assume such a choice, and refer to *the* radius of a plane.

B. An explicit solution for the HRT surface location

Without loss of generality, we will bound the time-derivative at $t = 0$ and use the shorthands $X_{t=0} = X$ and $R_{t=0} = R$. Since R is a strip contained in a canonical time slice of Minkowski on the boundary, and since the bulk spacetime has planar symmetry, there exists a homology hypersurface $\hat{\Sigma}$ of X respecting the planar symmetry—see Fig. 1. We can pick coordinates on $\hat{\Sigma}$ so that its induced metric $H_{\alpha\beta}$ reads

$$H_{\mu\nu}\mathrm{d}y^{\mu}\mathrm{d}y^{\nu} = B(r)\mathrm{d}r^2 + r^2(\mathrm{d}\phi^2 + \mathrm{d}\boldsymbol{x}^2),$$
$$r \in [r_0, \infty), \phi \in [-\Phi(r), \Phi(r)], \tag{30}$$

where $\phi = \Phi(r)$ is the coordinate embedding function of (half of) the HRT surface in $\hat{\Sigma}$, as illustrated in Fig. 1. r_0 is the smallest value of r probed by the HRT surface, corresponding to its tip. $\hat{\Sigma}$ can naturally be extended to include all $\phi \in \mathbb{R}$ by planar symmetry, and this choice turns out to be convenient for us. We denote the corresponding hypersurface as Σ, and refer to it as the extended homology hypersurface [105]. See Fig. 1. The boundary of Σ (in the bulk proper) is a plane of radius r_0.

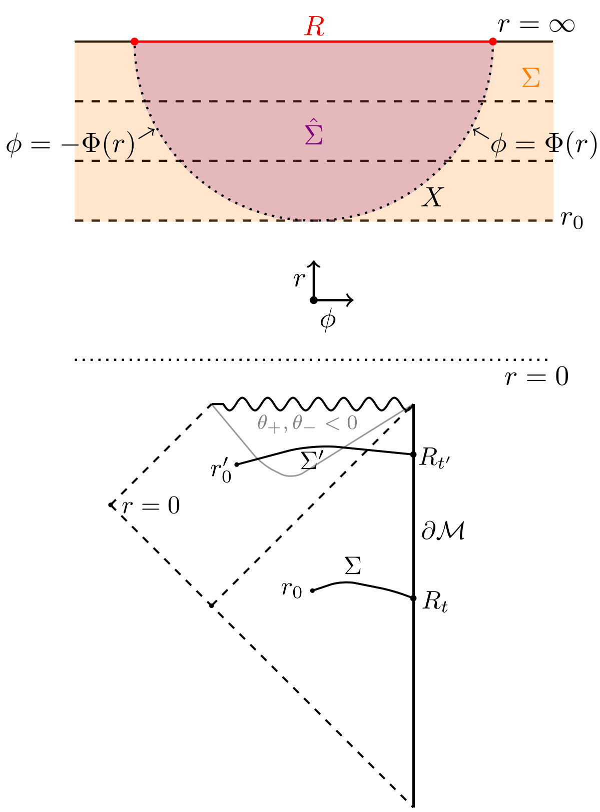

FIG. 1. Top: the planar symmetric homology hypersurface $\hat{\Sigma}$ with respect to the HRT surface X. Σ is the extended homology hypersurface, whose boundary is the plane at $r = r_0$. Dashed lines are planes—i.e. constant r surfaces. Bottom: example conformal diagram indicating possible embeddings of two extended homology hypersurfaces Σ and Σ'. The grey line is an apparent horizon, with vanishing outward null expansion, $\theta_+ = 0$.

Relying on the formulas derived in the remainder of this section, we prove the following technical Lemma in Appendix A 6:

Lemma 1. Let Σ be the extended homology hypersurface of an HRT surface X anchored at a strip region given by (18). Then a single coordinate system of the form

$$\mathrm{d}s^2 = B(r)\mathrm{d}r^2 + r^2\mathrm{d}\boldsymbol{x}^2 \tag{31}$$

is enough to cover all of Σ. Furthermore, X has only one turning point, meaning that embedding function $r(\phi)$ is monotonically increasing for $\phi \geq 0$.

This means one function $\Phi(r)$ contains all the information about the embedding of X in Σ—we do not need multiple branches. It also means that Σ cannot have any locally stationary planes—that is, no planes of vanishing mean curvature, where $B(r)$ would blow up [106]. The means we never need to worry about patching across coordinate systems when working on Σ. Geometrically, it implies that Σ has no "throats," i.e. locally minimal planes.

Now, taking $(r, \boldsymbol{x})$ to be coordinates on X, the induced metric on X reads

$$\mathrm{d}s^2|_X = [B(r) + r^2\Phi'(r)^2]\mathrm{d}r^2 + r^2\mathrm{d}\boldsymbol{x}^2. \tag{32}$$

Since X is an extremal surface, its area is stationary under all variations, including under variations within Σ. Enforcing this gives an ODE for $\Phi(r)$ in terms of $B(r)$. To find it, we compute the mean curvature $\mathcal{K}$ of X viewed as a submanifold of Σ and demand it to be zero. This gives the equation (see Appendix A 1 for a computation)

$$rB\Phi'' + (d-1)r^2(\Phi')^3 + \Phi'\left(dB - \frac{r}{2}B'\right) = 0. \tag{33}$$

The relevant boundary conditions are

$$\Phi'(r_0) = \infty, \qquad \Phi(r_0) = 0, \tag{34}$$

where the former says that r_0 is the radius of the plane tangent to the tip of the HRT surface (i.e. where $\frac{\mathrm{d}r}{\mathrm{d}\phi} = 0$), while the latter implements that $\phi = 0$ corresponds to the center of the strip. It turns out that Eq. (33) can be integrated, and the unique solution with the correct boundary condition is (see Appendix A 3)

$$\Phi(r) = \int_{r_0}^{r} \mathrm{d}\rho \frac{\sqrt{B(\rho)}}{\rho\sqrt{(\rho/r_0)^{2d-2} - 1}}. \tag{35}$$

This gives the location of the HRT surface within Σ explicitly in terms of the geometry of Σ. We now use this solution to determine the Einstein constraint equations on Σ, and to derive a formula for the rate of change of the entanglement growth.

C. A momentum-entanglement correspondence

Since X_t is extremal, its first order variation reduces to a pure boundary term given by (see for example the Appendix of [104,107]):

$$\left.\frac{\mathrm{dArea}[X_t]}{\mathrm{d}t}\right|_{t=0} = \int_{\partial X} N^a \eta_a, \tag{36}$$

where η^a is the translation vector generating the flow of ∂X_t at conformal infinity at $t = 0$, while N^a is the normal to ∂X that is also tangent to X, and that points toward the conformal boundary. In writing this formula, we implicitly assume that it is evaluated with some near-boundary cutoff that is subsequently removed. As is well known, given some choice of boundary conformal frame, a canonical choice of cutoff exists [108–110], which in our case reduces to a cutoff in the radial coordinate r. With a cutoff adapted to the Minkowski conformal frame and the falloffs (16) and (36) is finite, even though $\mathrm{Area}[X_t]$ diverges.

Now we write (36) in a more useful form. We will give all the main steps, but relegate tedious but straightforward computations to the Appendix.

Using the planar symmetry of Σ, the extrinsic curvature $K_{\alpha\beta}$ of Σ is given by

$$K_{\mu\nu}\mathrm{d}y^\mu \mathrm{d}y^\nu = K_{rr}(r)\mathrm{d}r^2 + K_{\phi\phi}(r)[\mathrm{d}\phi^2 + \mathrm{d}\boldsymbol{x}^2], \tag{37}$$

where we take the extrinsic curvature to be defined with respect to the future directed normal. Using this, we show in Appendix A 4, retracing the steps of [106], that

$$\left.\frac{\mathrm{dArea}[X_t]}{\mathrm{d}t}\right|_{t=0} = -\frac{\mathrm{Area}[\partial R]}{L^{d-2}} \lim_{r\to\infty} r^{d-3} K_{\phi\phi}. \tag{38}$$

Physically, $\lim_{r\to\infty} r^{d-3} K_{\phi\phi}$ measures the boost angle at which X hits the conformal boundary, or rather, the subleading part of the angle, since extremality implies that X hits $\partial\mathcal{M}$ orthogonally. This can be seen by studying extremal surfaces in a near-boundary expansion. Thus, we see that the entanglement growth is, up to a factor, identically given by the (subleading) boost angle at which the HRT surface hits the boundary. The same was found for extremal codimension-1 hypersurfaces in [106].

Next we want to find a more explicit expression for $\lim_{r\to\infty} r^{d-3} K_{\phi\phi}$. To do this, we need to use the Einstein constraint equations, which read

$$\mathcal{R} + K^2 - K^{\alpha\beta}K_{\alpha\beta} + \frac{d(d-1)}{L^2} = 16\pi G_N \mathcal{T}_{ab} t^a t^b,$$
$$D_\alpha K^\alpha{}_\beta - D_\beta K = 8\pi G_N \mathcal{T}_{ab} t^a e^b_\beta, \tag{39}$$

where $\mathcal{R}$ is the Ricci scalar of the metric on Σ, t^a the future unit normal to Σ, $K = H^{\alpha\beta}K_{\alpha\beta}$, and e^a_α a set of tangent vectors to Σ. To write these equations in coordinate form, it is convenient to introduce the function $\omega(r)$ as

$$B(r) = \frac{1}{\frac{r^2}{L^2} - \frac{\omega(r)}{r^{d-2}}}. \tag{40}$$

We will call $\omega(r)$ the Riemannian Hawking mass [111]. It will play a central role in our work. Whether or not $\omega(\infty)$ is proportional to the spacetime mass for some general spacelike hypersurface Σ depends on the behavior of the extrinsic curvature Σ at large r. It turns out that for $d \geq 3$, and with Σ being the extended homology hypersurface of an HRT surface, it has the property that it is proportional to the CFT energy density:

$$\langle T_{tt} \rangle = \frac{d-1}{16\pi G_N L^{d-1}} \omega(\infty), \qquad d \geq 3. \tag{41}$$

For $d = 2$, the right hand side is a lower bound on $\langle T_{tt}\rangle - \langle T_{tt}\rangle_{\mathrm{vac}}$, where the vacuum energy must be subtracted when we allow ϕ to be periodic. We will explain these facts in Sec. II E.

To get the constraints in a more manageable form, it is also convenient to write $K_{rr}(r)$ in terms of a function $F(r)$ which is the rr-component of the extrinsic curvature in an orthonormal basis,

$$K_{rr}(r) \equiv B(r)F(r). \tag{42}$$

In terms of these functions, the constraint equations in coordinate form read

$$(d-1)\frac{\omega'(r)}{r^{d-1}} = 2\mathcal{E}(r) - \frac{(d^2-3d+2)}{r^4} K_{\phi\phi}(r)^2$$
$$- \frac{2(d-1)}{r^2} F(r) K_{\phi\phi}(r), \tag{43}$$

$$K'_{\phi\phi}(r) - \frac{K_{\phi\phi}(r)}{r} = rF(r) - \frac{r^2}{d-1}\mathcal{J}(r), \tag{44}$$

where we introduced the notation

$$\mathcal{E} = 8\pi G_N \mathcal{T}_{ab} t^a t^b,$$
$$\mathcal{J} = 8\pi G_N \mathcal{T}_{ab} (\partial_r)^a t^b. \tag{45}$$

These are proportional to the energy density and radial momentum density of the matter with respect to the frame t^a. $\mathcal{J} > 0$ corresponds to matter falling into the bulk toward smaller r. From (16) and the fact that $B(r) \sim \mathcal{O}(r^{-1})$, we find that

$$\mathcal{E} \sim o(1/r^d), \qquad \mathcal{J} \sim o(1/r^{d+1}), \tag{46}$$

where we use that $\frac{1}{\sqrt{B}}(\partial_r)^a$ is a unit vector.

To turn (43) and (44) into a closed system, we will eliminate $F(r)$. We do this by imposing extremality of X in the direction of t^a. To do this, note that the inward (outward) null expansion θ_+ (θ_-) of X can be written as (see for example the Appendix of [106])

$$\sqrt{2}\theta_\pm[X] = \pm\mathcal{K}[X] + K - n^\alpha n^\beta K_{\alpha\beta}, \tag{47}$$

where n^α is the outward normal to X within Σ [116], and where we remind that $\mathcal{K}[X]$ is the mean curvature of X within Σ. Extremality means $\theta_+ = \theta_- = 0$, which implies that $\mathcal{K} = 0$ and

$$K|_X = n^\alpha n^\beta K_{\alpha\beta}|_X. \tag{48}$$

This equation holds at $\phi = \Phi(r)$, which by planar symmetry means it holds everywhere on Σ. Writing out this equation in coordinates, carried out in Appendix A 2, we find

$$F + \frac{(d-2)K_{\phi\phi}}{r^2} + (d-1)K_{\phi\phi}\frac{(\Phi')^2}{B} = 0. \tag{49}$$

Plugging in the solution for $\Phi(r)$, given in (35), we get that

$$F(r) = -\frac{K_{\phi\phi}(r)}{r^2}\left(\frac{(d-2)r^{2d-2} + r_0^{2d-2}}{r^{2d-2} - r_0^{2d-2}}\right), \tag{50}$$

which upon insertion into the constraints, gives a closed system of ODEs for the functions $\omega, K_{\phi\phi}$:

$$\frac{\omega'(r)}{r^{d-1}} = \frac{2}{d-1}\mathcal{E}(r) + \frac{K_{\phi\phi}^2}{r^4}h_1(r), \tag{51}$$

$$K'_{\phi\phi}(r) + \frac{K_{\phi\phi}}{r}h_2(r) = -\frac{r^2}{d-1}\mathcal{J}(r), \tag{52}$$

where

$$h_1(r) = \frac{(d-2)(r/r_0)^{2d-2} + d}{(r/r_0)^{2d-2} - 1},$$
$$h_2(r) = \frac{(d-3)(r/r_0)^{2d-2} + 2}{(r/r_0)^{2d-2} - 1}. \tag{53}$$

Now, $F(r)$ is a component of the extrinsic curvature in an orthonormal basis, so it must be finite at r_0. Using this to fix an integration constant, we find that the solutions of (51) and (52) are

$$K_{\phi\phi}(r) = -\frac{r^2}{(d-1)\sqrt{(r/r_0)^{2d-2} - 1}} \tag{54}$$

$$\times \int_{r_0}^{r} \mathrm{d}\rho\,\mathcal{J}(\rho)\sqrt{(\rho/r_0)^{2d-2} - 1}, \tag{55}$$

$$\omega(r) = \omega(r_0) \tag{56}$$

$$+ \int_{r_0}^{r} \mathrm{d}\rho\left[\rho^{d-5}h_1(\rho)K_{\phi\phi}(\rho)^2 + \frac{2\rho^{d-1}}{d-1}\mathcal{E}(\rho)\right], \tag{57}$$

where $K_{\phi\phi}(r_0) = 0$ follows from boundedness of the matter momentum density $\mathcal{J}(\rho)$ [117]. Inserting (55) into (38) and multiplying by $(4G_N)^{-1}$, we get that

$$\left.\frac{\mathrm{d}S_R}{\mathrm{d}t}\right|_{t=0} = \frac{\mathrm{Area}[\partial R]}{4G_N L^{d-2}(d-1)}\int_{r_0}^{\infty}\mathrm{d}r\,\mathcal{J}(r)\sqrt{r^{2d-2} - r_0^{2d-2}}. \tag{58}$$

Since $\mathcal{J} > 0$ corresponds to a flux of energy density toward decreasing r, we see that matter falling out of the entanglement wedge and deeper into the bulk is directly responsible for the increase of entanglement. Conversely, outgoing matter is responsible for decrease in entanglement. We can also rewrite this formula in a covariant way. In Appendix A 4 we show that

$$\left.\frac{\mathrm{d}S_R}{\mathrm{d}t}\right|_{t=0} = \int_X G\mathcal{T}_{ab}n^a t^a, \tag{59}$$

where n^a is the outward unit normal to X that is tangent to Σ, and

$$G(r) = \frac{2\pi r^d}{(d-1)r_0^{d-1}}. \tag{60}$$

The formulas (38) and (55)–(60) are the main results of this section. These results together with the theorems proven in the following section are crucial pieces to our proven bounds.

D. Geometric constraints on the HRT surface

In this section, we prove the following result, while will be used to get our final bounds:

Theorem 4. Let $(\mathcal{M}, g_{ab})$ be a regular asymptotically $\mathrm{AdS}_{d+1\geq 3}$ spacetime with planar symmetry satisfying the DEC. Let X be the HRT surface of a strip R of width ℓ, and let be r_0 be the smallest radius probed by X. Then

$$\frac{L^2}{r_0} \leq \frac{\Gamma\left(\frac{1}{2(d-1)}\right)}{2\sqrt{\pi}\Gamma\left(\frac{d}{2(d-1)}\right)}\ell. \tag{61}$$

Furthermore, if $r_{0,\mathrm{vac}}$ is the smallest radius probed by the HRT surface X_0 of a strip of width ℓ in pure AdS_{d+1}, then

$$r_0 \geq r_{0,\mathrm{vac}}. \tag{62}$$

We now give the proof assuming that $\omega(r_0) \geq 0$, and then we will spend most of the rest of this section proving this assertion.

Proof. By Lemma 3, proven below, we have that $\omega(r_0) \geq 0$. Furthermore, the DEC implies that $\mathcal{E}$ is positive. Hence, (57) gives that $\omega(r)$ is everywhere positive. But this means that

$$B(r) = \frac{1}{\frac{r^2}{L^2} - \frac{\omega(r)}{r^{d-2}}} \geq \frac{L^2}{r^2}, \tag{63}$$

which allows us to lower bound the strip width as follows:

$$\begin{aligned} \ell &= 2L\Phi(\infty) = 2L\int_{r_0}^{\infty} \mathrm{d}\rho \frac{\sqrt{B(\rho)}}{\rho\sqrt{(\rho/r_0)^{2d-2}-1}} \\ &\geq 2L^2 \int_{r_0}^{\infty} \mathrm{d}\rho \frac{1}{\rho^2\sqrt{(\rho/r_0)^{2d-2}-1}} \\ &= \frac{2L^2}{r_0}\frac{\sqrt{\pi}\Gamma\left(\frac{d}{2(d-1)}\right)}{\Gamma\left(\frac{1}{2(d-1)}\right)}. \end{aligned} \tag{64}$$

Finally, if we are in pure AdS, we must have that the spacetime mass is vanishing, implying that $\omega(\infty) = 0$, and so by $\omega'(r) \geq 0$ and the fact that $\omega(r_0) \geq 0$, we must have $\omega(r) = 0$ everywhere. But that means that the above inequalities become equalities, giving $\frac{L^2}{r_0} \geq \frac{L^2}{r_{0,\mathrm{vac}}}$, which implies (62). ■

Now we turn to proving that $\omega(r_0)$ is non-negative. The crucial tool is a planar-symmetric AdS_{d+1} version of the Lorentzian Hawking mass [118], which we define for a planar surface σ as

$$\mu[\sigma] = \frac{r^d}{L^2} - \frac{2r^d\theta_+\theta_-}{k_+ \cdot k_-(d-1)^2}, \tag{65}$$

where k^+ and k^- are the outward and inward null vectors orthogonal to σ, respectively, and $\theta_\pm$ the corresponding null expansions. In [119], generalizing the results of [120] to planar symmetry and AAdS_{d+1} spacetimes, it was shown that the DEC implies that $\mu[\sigma]$ is monotonically non-decreasing when σ is moving in an outward spacelike direction, provided we are in a normal region of spacetime, meaning that $\theta_+ \geq 0, \theta_- \leq 0$ when we take k_+^a and k_-^a to be future directed [121].

Furthermore, it is useful to rewrite the Riemannian Hawking mass $\omega(r)$ in a different way. ω can be thought of as a function of a planar surface σ together with a hypersurface Σ containing it, and in [106] it is shown that we can write ω as

$$\omega[\sigma,\Sigma] = \frac{r^d}{L^2} - \frac{\mathcal{K}[\sigma]^2}{(d-1)^2}, \tag{66}$$

where $\mathcal{K}$ is the mean curvature of σ in Σ. Using (47), which assumes the normalization $k_+ \cdot k_- = -1$, we see that $2\theta_+\theta_- = (K - n^\alpha n^\beta K_{\alpha\beta})^2 - \mathcal{K}^2$, and so we get the following relation between the Hawking masses

$$\mu[\sigma] = \omega[\sigma,\Sigma] + \frac{r^d}{(d-1)^2}(K - n^\alpha n^\beta K_{\alpha\beta})^2. \tag{67}$$

With this in hand, we prove the following Lemma.

Lemma 2. Let Γ be a complete planar symmetric hypersurface with one conformal boundary. Let σ_r be a one-parameter family of planes in Γ with radius r, and with $r \in (0,\epsilon]$ for any $\epsilon > 0$. Then

$$\lim_{r\to 0}\mu[\sigma_r] \geq 0. \tag{68}$$

Proof. Let us pick coordinates

$$\mathrm{d}s^2|_\Gamma = \left[\frac{r^2}{L^2} - \frac{\omega(r)}{r^{d-2}}\right]^{-1}\mathrm{d}r^2 + r^2\mathrm{d}\boldsymbol{x}^2 \tag{69}$$

on Γ in a neighborhood of $r = 0$. Since Γ is complete and we only have one conformal boundary, arbitrarily small r must be part of Γ. Since Γ is spacelike, we must have $\omega(r) \leq r^d/L^2$, which means that $\omega(r) \sim \mathcal{O}(r^d)$ at small r. Now, from (67) we see that $\mu[\sigma_r] \geq \omega[\sigma_r,\Gamma]$ and so

$$\mu[\sigma_r] \geq \mathcal{O}(r^d). \tag{70}$$

Taking $r \to 0$ proves our assertion. ■

Now we are ready to prove that $\omega(r_0) \geq 0$. The proof will also teach us that the tip of the HRT surface cannot lie in a trapped region, which itself is an interesting result.

Lemma 3. Let $(\mathcal{M}, g_{ab})$ be a planar-symmetric regular asymptotically AdS_{d+1} spacetime. Let X be the HRT surface of a strip. Then the tip of X lies in an untrapped region of spacetime, meaning the future null expansions of the plane σ tangent to X at the tip satisfies

$$\theta_+[\sigma] \geq 0, \qquad \theta_-[\sigma] \leq 0. \tag{71}$$

Furthermore, if the DEC holds and $(\mathcal{M}, g)$ is regular, the Riemannian Hawking mass of σ is non-negative:

$$\omega[\sigma,\Sigma] = \omega(r_0) \geq 0. \tag{72}$$

Proof. Let Σ be the unique planar symmetric extended homology hypersurface containing X. Let σ be the boundary of Σ in the bulk, having radius r_0. Its null expansion is

$$\sqrt{2}\theta_\pm[\sigma] = \pm\mathcal{K}[\sigma] + K - r^\alpha r^\beta K_{\alpha\beta}, \tag{73}$$

where $r^\alpha = \frac{1}{\sqrt{B}}(\partial_r)^\alpha$. An explicit computation gives

$$\mathcal{K}[\sigma] = \frac{d-1}{r_0\sqrt{B(r_0)}},$$
$$K = \frac{1}{B}K_{rr} + \frac{K_{\phi\phi}(d-1)}{r^2}, \tag{74}$$

and so we find

$$\sqrt{2}\theta_\pm[\sigma] = \pm\frac{d-1}{r_0\sqrt{B(r_0)}} - \frac{K_{\phi\phi}(r_0)(d-1)}{r_0^2}. \tag{75}$$

From (55) we have that $K_{\phi\phi}(r_0) = 0$, and so we get that

$$\pm\theta_\pm \geq 0, \tag{76}$$

proving the first assertion.

Next, since $K_{\phi\phi}(r_0) = 0$ we see that $2\theta_+\theta_-|_\sigma = -\mathcal{K}^2|_\sigma$, implying that $\mu[\sigma] = \omega[\sigma, \Sigma]$. Now, since our spacetime is AdS-hyperbolic, we can embed σ in a complete hypersurface with planar symmetry Γ, see Fig. 2. Since σ lies in an untrapped region of spacetime, and since Γ is spacelike, $\mu[\sigma]$ is monotonically nonincreasing as we deform σ in inward along Γ while preserving its planar symmetry. Since the g_{ab} is C^2, $\theta_\pm$ are continuous, and so as we deform σ inward, one of two things happen. Either we hit a marginally trapped surface, where $\theta_+\theta_- = 0$ and where μ is manifestly positive, or we approach $r = 0$, where we again have that μ is non-negative by Lemma 2. See Fig. 2. But since μ is nonincreasing along this deformation, and since it ends up somewhere non-negative, we must have $\mu[\sigma] \geq 0$. But $\mu[\sigma] = \omega[\sigma, \Sigma]$, completing the proof. ■

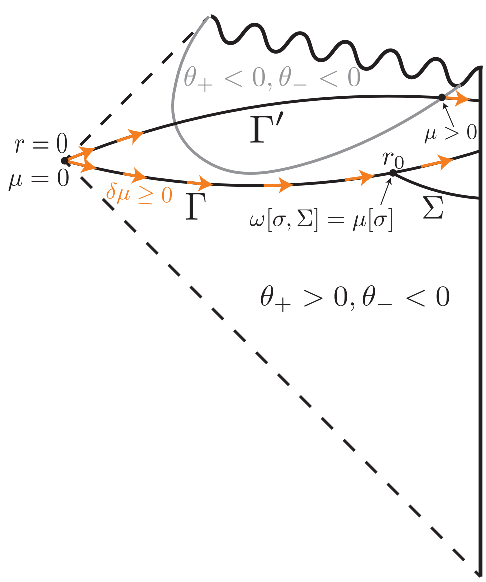

FIG. 2. Example of two complete hypersurfaces Γ and Γ'. The Lorentzian Hawking mass is vanishing at $r = 0$ and positive at marginally trapped surfaces, given by the planes contained in the gray line. μ is monotonically nondecreasing along spacelike outward flows in the untrapped region, where $\theta_+ \geq 0, \theta_- \leq 0$. At the boundary σ of the extended homology hypersurface Σ, the Riemannian Hawking mass ω with respect to Σ agrees with the Lorentzian Hawking mass μ.

We have illustrated the fact that the tip cannot lie in a trapped region of spacetime in Fig. 1—the tip cannot lie behind the gray line. Note that the proof of this fact does not rely on the DEC. This result improves on the findings of [123] in the special case where we have planar symmetry. In [123], they showed without any symmetry assumptions that the tip of an HRT surface in a $(2+1)$–dimensional spacetime can never lie in the so-called umbral region, which is a special subset of the trapped region that lies behind regular holographic screens [123,124]. They also showed this result with planar symmetry in all dimensions. Here we extend this result to show that the whole trapped region is forbidden, although our result is more limited in that it always requires planar symmetry and a strip (or spherical) boundary region. Note also that this result does not forbid X to probe inside trapped regions—it is only the tip that is forbidden to lie there (see Fig. 1). For example, for early times after a quench, the HRT surface will have portions threading through the trapped region [33,34].

E. Proofs

1. Proof of $d = 2$ entropy bound

We are now ready to prove Theorem 1. Evaluating the Lorentzian Hawking mass on a sphere at large r in a planar symmetric AAdS_{d+1} spacetime with falloffs (16), we get that

$$\langle T_{tt}\rangle = \frac{d-1}{16\pi G_N L^{d-1}}\mu(\infty). \tag{77}$$

This is valid also for $d = 2$, except if ϕ is periodically identified, we must replace the left-hand side with $\langle T_{tt}\rangle - \langle T_{tt}\rangle_{\mathrm{vac}}$. It can readily be seen to be true by evaluating $\mu(\infty)$ near the boundary in the usual Fefferman-Graham expansion [108–110]. Now, from (67) and (74) we have that

$$\mu(r) = \omega(r) + r^{d-4}K_{\phi\phi}(r)^2. \tag{78}$$

From (55), we see that $K_{\phi\phi}$ has asymptotic falloff $K_{\phi\phi} \sim \mathcal{O}(r^{3-d})$. Thus, we get that for $d \geq 3$, $\mu(\infty) = \omega(\infty)$, while for $d = 2$, we have

$$\mu(\infty) = \omega(\infty) + (\lim_{r\to\infty} r^{-1}K_{\phi\phi})^2. \tag{79}$$

Since $\omega(\infty) \geq 0$ by the DEC, when $d = 2$ we obtain

$$|\lim_{r\to\infty} r^{-1}K_{\phi\phi}| \le \sqrt{\mu(\infty)} = \sqrt{16\pi G_N L\langle T_{tt}\rangle}. \quad (80)$$

Using that $\mathrm{Area}[\partial R_t] = 2$, and combining (80) and (38) then yields

$$\left|\frac{\mathrm{d}S_R}{\mathrm{d}t}\right|_{t=0} \le \frac{1}{2G_N}\sqrt{16\pi G_N L\langle T_{tt}\rangle} = \sqrt{\frac{8\pi c}{3}\langle T_{tt}\rangle}, \quad (81)$$

where we used the known Brown-Henneaux expression for the central charge: $c = \frac{3L}{2G_N}$ [125]. This proves Theorem 1.

2. Proof of $d=2$ correlator bound

The above result also implies a bound on correlators that can be computed using the geodesic approximation, since in $d=2$ the HRT surfaces are just geodesics. The geodesic approximation says that the two-point function of a CFT scalar operator O of large scaling dimension $\Delta \gg 1$ can be computed as

$$\langle O(\boldsymbol{x})O(0)\rangle_{\rho(t)} = \eta e^{-\frac{\Delta}{L}\|X_t\|_{\mathrm{reg}}}, \quad (82)$$

where η is some constant, and $\|X_t\|_{\mathrm{reg}}$ is the regularized distance of a geodesic anchored at the points $(t,\boldsymbol{x})$ and $(t,0)$ on the conformal boundary. We here adopted the Schrödinger picture. Combining (38), (80), and (82), we get

$$\left|\frac{\mathrm{d}}{\mathrm{d}t}\log\langle O(x)O(0)\rangle_{\rho(t)}\right| \le \sqrt{\frac{96\pi\Delta^2}{c}\langle T_{tt}\rangle}, \qquad d=2. \quad (83)$$

3. Proof of bounds for small ℓ

Now let us consider the result for small subregions, given by Theorem 3. The following Lemma is what we need:

Lemma 4. Let $(\mathcal{M}, g_{ab})$ be a regular asymptotically $\mathrm{AdS}_{d+1\ge 3}$ spacetime with planar symmetry satisfying the DEC. Let X be the HRT surface of a strip R of width ℓ, and let be r_0 be the smallest radius probed by X. Assume that

$$\frac{\ell^d\langle T_{tt}\rangle}{c_{\mathrm{eff}}} \ll 1. \quad (84)$$

Then

$$|\lim_{r\to\infty} r^{d-3}K_{\phi\phi}| \le \frac{L}{2r_0}\omega(\infty)\left[1 + \mathcal{O}\left(\frac{\ell^d\langle T_{tt}\rangle}{c_{\mathrm{eff}}}\right)\right]. \quad (85)$$

Proof. Let us for convenience define $W = -\lim_{r\to\infty} r^{d-3}K_{\phi\phi}$, and assume without loss of generality that $W > 0$ (otherwise, just reverse the time direction). Using the solutions (55) and (57), we have that

$$\begin{aligned}\frac{(d-1)W}{\omega(\infty)} &= \frac{\int_{r_0}^{\infty}\mathrm{d}r\mathcal{J}(r)\sqrt{r^{2d-2}-r_0^{2d-2}}}{\omega(r_0) + \int_{r_0}^{\infty}\mathrm{d}r\left[r^{d-5}h_1(r)K_{\phi\phi}(r)^2 + \frac{2r^{d-1}}{d-1}\mathcal{E}(r)\right]}\\ &\le \frac{(d-1)\int_{r_0}^{\infty}\mathrm{d}r r^{d-1}\mathcal{J}(r)}{2\int_{r_0}^{\infty}\mathrm{d}r r^{d-1}\mathcal{E}(\rho)}. \end{aligned}\quad (86)$$

The DEC requires that

$$0 \le 8\pi G_N \mathcal{T}_{ab}\left[t^a \pm \frac{1}{\sqrt{B}}(\partial_r)^a\right]t^b = \mathcal{E} \pm \frac{1}{\sqrt{B}}\mathcal{J}, \quad (87)$$

and so we have that

$$\mathcal{E} \ge \frac{1}{\sqrt{B}}|\mathcal{J}|. \quad (88)$$

Writing B in terms of ω, and enforcing the DEC, we get

$$\frac{W}{\omega(\infty)} \le \frac{\int_{r_0}^{\infty}\mathrm{d}r r^{d-1}\mathcal{J}(r)}{\frac{2}{L}\int_{r_0}^{\infty}\mathrm{d}r r^d\sqrt{1-\frac{\omega(r)L^2}{r^d}}|\mathcal{J}(r)|}. \quad (89)$$

Let us now for a moment assume that we are perturbatively close to the vacuum, where ϵ is a perturbative parameter parametrizing the magnitude of $\omega(\infty)$. By monotonicity and positivity of $\omega(r)$, $\omega(r) \sim \mathcal{O}(\epsilon)$ as well, and so the $\omega(r)$ appearing in the square root gives higher order contributions:

$$\begin{aligned}\frac{W}{\omega(\infty)} &\le \frac{\int_{r_0}^{\infty}\mathrm{d}r r^{d-1}|\mathcal{J}(r)|}{\frac{2}{L}\left[\int_{r_0}^{\infty}\mathrm{d}r r^d|\mathcal{J}(r)| - \frac{L^2}{2}\int_{r_0}^{\infty}\mathrm{d}r\omega(r)|\mathcal{J}(r)| + \ldots\right]}\\ &= \frac{L}{2}\frac{\int_{r_0}^{\infty}\mathrm{d}r r^{d-1}|\mathcal{J}(r)|}{\int_{r_0}^{\infty}\mathrm{d}r r^d|\mathcal{J}(r)|}\left[1 + \frac{L^2}{2}\frac{\int_{r_0}^{\infty}\mathrm{d}r\omega(r)|\mathcal{J}|}{\int_{r_0}^{\infty}\mathrm{d}r r^d|\mathcal{J}|} + \ldots\right]\\ &\le \frac{L}{2r_0}\left[1 + \frac{L^2}{r_0^d}\omega(\infty) + \ldots\right]\\ &\le \frac{L}{2r_0}\left[1 + \frac{L^{2d}}{r_0^d}\frac{\mu(\infty)}{L^{2d-2}} + \ldots\right]\\ &= \frac{L}{2r_0}\left[1 + \frac{16\pi\eta_d}{d-1}\frac{\ell^d\langle T_{tt}\rangle}{c_{\mathrm{eff}}} + \ldots\right], \end{aligned}\quad (90)$$

where η_d is the $O(1)$ number coming from using (61). We see that the effective expansion parameter is the dimensionless quantity $\frac{\ell^d\langle T_{tt}\rangle}{c_{\mathrm{eff}}}$. So the expansion is not really in small mass, which is dimensionful, but in small strip width relative to the inverse energy density per CFT degree of freedom. Either way, we obtain (85). ■

From (38) and (61), we get, up to the perturbative corrections,

$$\begin{aligned}\left|\frac{\mathrm{d}S_R}{\mathrm{d}t}\right| &\leq \frac{\mathrm{Area}[\partial R]}{4G_N L^{d-2}}\frac{L}{2r_0}\omega(\infty)\\ &\leq \frac{\sqrt{\pi}}{d-1}\frac{\Gamma(\frac{1}{2(d-1)})}{\Gamma(\frac{d}{2(d-1)})}\ell\mathrm{Area}[\partial R]\langle T_{tt}\rangle\\ &= \mathrm{Vol}[R]\langle T_{tt}\rangle\begin{cases}2\pi & d=2\\ \frac{\sqrt{\pi}}{d-1}\frac{\Gamma(\frac{1}{2(d-1)})}{\Gamma(\frac{d}{2(d-1)})} & d>2\end{cases},\end{aligned}\tag{91}$$

where we used (41) and (61) in the second inequality. This also holds for $d=2$, since $\omega(\infty)\leq\mu(\infty)$, provided we replace $\langle T_{tt}\rangle\to\langle T_{tt}\rangle-\langle T_{tt}\rangle_{\mathrm{vac}}$ if ϕ is compact. Also, note that for $d=2$ we have that $\ell\mathrm{Area}[\partial R]=2\mathrm{Vol}[R]$. This completes the proof of Theorem 3 for strip regions.

These computations also gives the $d=2$ bound on equal-time correlators for small separation. Combining (82) with (36) and (85), we get

$$\left|\frac{\mathrm{d}}{\mathrm{d}t}\log\langle O(x)O(0)\rangle_{\rho(t)}\right|\leq\frac{12\pi\Delta|x|}{c}\langle T_{tt}\rangle \times[1+\mathcal{O}(x^2\langle T_{tt}\rangle/c)].\tag{92}$$

4. Proof of bounds in thin-shell spacetimes

We now turn our attention to thin-shell spacetimes, to prove Theorem 2. Furthermore, we will be able to establish a bound of the form $|\partial_t S|\leq\#\mathrm{Vol}[R]\langle T_{tt}\rangle$ that holds for any ℓ.

Consider a spacetime where the matter consists of a single thin shell of matter that separately satisfies the DEC, together with a possible contribution from any number of $U(1)$ gauge fields:

$$\begin{aligned}\mathcal{E}&=\kappa\delta(r-\hat{r})+\mathcal{E}^{\mathrm{Maxwell}},\\ \mathcal{J}&=\eta\delta(r-\hat{r}),\end{aligned}\tag{93}$$

for some $\eta,\kappa,\hat{r}>r_0$. See Fig. 3. Here we used that in planar symmetry, Maxwell fields give no contribution to the radial momentum density $\mathcal{J}$ (see for example Sec. 3 of [106]).

The DEC, through (88), imposes that $\mathcal{J}$ only can have support at $\hat{r}$. Without loss of generality, we take $\eta>0$. Let us in this section also use our scaling freedom in r to set $r_0=L$ and choice of units to set $L=1$.

Define again $W=-\lim_{r\to\infty}r^{d-3}K_{\phi\phi}$. Plugging (93) into (55), the solution for $K_{\phi\phi}$ is

$$K_{\phi\phi}(r)=-\frac{r^2}{d-1}\eta\sqrt{\frac{\hat{r}^{2d-2}-1}{r^{2d-2}-1}}\theta(r-\hat{r}),\tag{94}$$

and so

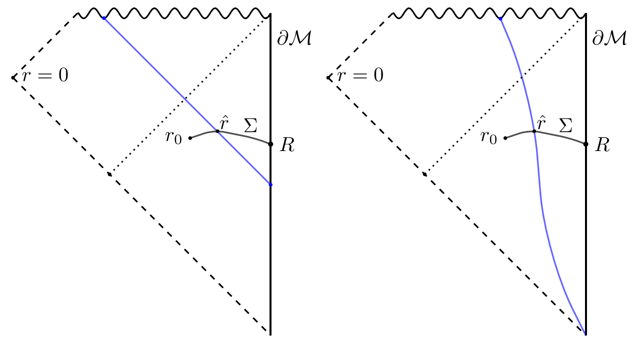

FIG. 3. Examples of thin-shell spacetimes, where the blue lines correspond to the shells. The left space is dual to a uniform quench, where matter is thrown in from the boundary, corresponding to injection of a large amount of energy into the CFT. The right is a spacetime with a shell of matter propagating purely in the bulk interior, while CFT energy is conserved for all times.

$$\eta=\frac{(d-1)W}{\sqrt{\hat{r}^{2d-2}-1}},\tag{95}$$

which gives

$$K_{\phi\phi}(r)=-\frac{r^2W}{\sqrt{r^{2d-2}-1}}\theta(r-\hat{r}).\tag{96}$$

Next, let us solve for the contribution to $\omega(r)$ from the squared extrinsic curvature term in (57):

$$\begin{aligned}Q(r)&\equiv\int_1^r\mathrm{d}\rho\rho^{d-5}K_{\phi\phi}(\rho)^2h_1(\rho)\\ &=\theta(r-\hat{r})W^2\int_{\hat{r}}^r\mathrm{d}\rho\rho^{d-1}\frac{h_1(\rho)}{[\rho^{2d-2}-1]}\\ &=W^2\theta(r-\hat{r})\left[\frac{\hat{r}^d}{\hat{r}^{2d-2}-1}-\frac{r^d}{r^{2d-2}-1}\right].\end{aligned}\tag{97}$$

To proceed, we need to understand what happens to ω as we cross the shock. Restricting attention to a small neighborhood of $\hat{r}$, where we can treat explicit occurrences of r not appearing in delta functions as constant, the equation for ω reads

$$(d-1)\frac{\omega'(r)}{\hat{r}^{d-1}}=2\mathcal{E}^{\mathrm{shell}}+\ldots,\tag{98}$$

where the terms indicated with dots will make no contribution to the discontinuity. Remembering that the DEC implies that $\sqrt{B}\mathcal{E}\geq|\mathcal{J}|$, imposing the DEC on the shell means that

$$\mathcal{E}^{\mathrm{shell}}\geq\sqrt{\hat{r}^2-\frac{\omega(r)}{\hat{r}^{d-2}}}\eta\delta(r-\hat{r}).\tag{99}$$

Inserting (99) into (98), dividing by the prefactor of the delta function, and integrating from $\hat{r}-\varepsilon$ to $\hat{r}+\varepsilon$ for some small positive ε, we find

$$\sqrt{\hat{r}^2-\frac{\omega_-}{\hat{r}^{d-2}}}-\sqrt{\hat{r}^2-\frac{\omega_+}{\hat{r}^{d-2}}}\geq\frac{\hat{r}}{d-1}\eta+\mathcal{O}(\varepsilon), \tag{100}$$

where we defined $\omega_\pm=\omega(\hat{r}\pm\varepsilon)$. We only have a sensible solution when $B(r)$ is real and positive everywhere, which requires

$$\frac{1}{d-1}\eta\leq\sqrt{1-\frac{\omega_-}{\hat{r}^d}}. \tag{101}$$

Solving for ω_- from (100) and inserting our expression for η, we get that

$$\omega_+\geq\omega_-+\frac{\hat{r}^d}{\sqrt{\hat{r}^{2d-2}-1}}W\left[\sqrt{1-\frac{\omega_-}{\hat{r}^d}}-\frac{W}{\sqrt{\hat{r}^{2d-2}-1}}\right]. \tag{102}$$

Using this and (78), the Lorentzian Hawking mass at infinity has the lower bound

$$\begin{aligned}\mu(\infty)&=\omega(\infty)+\delta_{d2}W^2\\&\geq\omega_-+\frac{\hat{r}^d}{\sqrt{\hat{r}^{2d-2}-1}}W\left[\sqrt{1-\frac{\omega_-}{\hat{r}^d}}-\frac{W}{\sqrt{\hat{r}^{2d-2}-1}}\right]\\&\quad+Q(\infty)+\delta_{d2}W^2\\&=\omega_-+\frac{\hat{r}^d}{\sqrt{\hat{r}^{2d-2}-1}}W\sqrt{1-\frac{\omega_-}{\hat{r}^d}},\end{aligned} \tag{103}$$

where δ_{ij} is the Kronecker delta. Thus, for any real n, we have that

$$\frac{W^n}{\mu(\infty)}\leq\frac{W^n}{\omega_-+\frac{\hat{r}^d}{\sqrt{\hat{r}^{2d-2}-1}}W\sqrt{1-\frac{\omega_-}{\hat{r}^d}}}\equiv U_n, \tag{104}$$

together with the constraints

$$0\leq\omega_-\leq\hat{r}^d, \tag{105}$$

$$W\leq\sqrt{\hat{r}^{2d-2}-1}\sqrt{1-\frac{\omega_-}{\hat{r}^d}}. \tag{106}$$

Our goal will now be to upper bound U_n for all legal triplets $(W,\hat{r},\omega_-)$ for $n=1$ and $n=\frac{d}{d-1}$, which turns out to be values that will give interesting growth bounds.

Note first that we have

$$\partial^2_{\omega_-}U_n\geq 0, \tag{107}$$

so any local extremum of U_n with respect to ω_- is a minimum. Thus, for any given W and $\hat{r}$, U_n is maximized when ω_- is on the boundary of its domain. First, take $\omega_-=0$. Then, assuming that $1\leq n\leq\frac{d}{d-1}$,

$$U_n=\frac{W^{n-1}\sqrt{\hat{r}^{2d-2}-1}}{\hat{r}^d}\leq\frac{[\hat{r}^{2d-2}-1]^{\frac{n}{2}}}{\hat{r}^d}\leq\frac{\hat{r}^{n(d-1)}}{\hat{r}^d}\leq 1, \tag{108}$$

where we used (106) in the second inequality. For $n=1$, we get the stronger bound

$$U_1\leq\frac{\sqrt{\hat{r}^{2d-2}-1}}{\hat{r}^d}\leq\sqrt{\frac{d-1}{d^{\frac{d}{d-1}}}}\equiv\alpha_d, \tag{109}$$

where the upper bound is found by maximizing with respect to $\hat{r}$. Next, let us look at the maximal value for ω_-, where we have the equality

$$W=\sqrt{\hat{r}^{2d-2}-1}\sqrt{1-\frac{\omega_-}{\hat{r}^d}}. \tag{110}$$

Neglecting the first ω_- in the denominator of U_n and using $W\leq\sqrt{\hat{r}^{2d-2}-1}$, we get

$$U_n\leq\frac{[\hat{r}^{2d-2}-1]^{n/2}}{\hat{r}^d}. \tag{111}$$

But this is just the expression bounded earlier, and so (108) and (109) holds generally. Restoring factors of L, r_0, we have the following true bounds

$$W\leq L^{\frac{d-2}{d}}\omega(\infty)^{\frac{d-1}{d}}, \tag{112}$$

$$W\leq\alpha_d\frac{L}{r_0}\omega(\infty). \tag{113}$$

Inserting (112) into (38), we find

$$\left|\frac{\mathrm{d}S_R}{\mathrm{d}t}\right|\leq\frac{1}{4}\mathrm{Area}[\partial R]c_{\mathrm{eff}}\left[\frac{16\pi}{(d-1)c_{\mathrm{eff}}}\langle T_{tt}\rangle\right]^{\frac{d-1}{d}}, \tag{114}$$

proving Theorem 2 for strip regions.

Next, redoing the steps in (91) with the numerical factor from in (113), we get the part of the following theorem concerning strips:

Theorem 5. Consider the same setup as in Theorem 2. Then

$$\left|\frac{\mathrm{d}}{\mathrm{d}t}\left(\frac{\mathrm{Area}[X_t]}{4G_N}\right)\right|\leq\kappa'_d\mathrm{Vol}[R]\langle T_{tt}\rangle, \tag{115}$$

with

$$\kappa'_d = \iota_d \begin{cases} 2\pi & R \text{ is an interval and } d = 2, \\ \sqrt{\frac{4\pi}{(d-1)}} & R \text{ is a strip and } d > 2, \\ \sqrt{16\pi(d-1)} & R \text{ is a ball and } d > 2. \end{cases}$$
$$\iota_d = d^{-\frac{d}{2(d-1)}} \frac{\Gamma\left(\frac{1}{2(d-1)}\right)}{\Gamma\left(\frac{d}{2(d-1)}\right)}. \tag{116}$$

The part concerning balls is proven in the next section. Now, for a strip, a few values of the prefactor κ'_d, together with the prefactor κ_d in the more general bound (8), is

$$\kappa_d = \begin{cases} 2\pi & d=2 \\ 2.62\ldots & d=3 \\ 2.43\ldots & d=4 \\ 2 & d=\infty \end{cases}, \quad \kappa'_d = \begin{cases} 2\pi & d=2 \\ 3.25\ldots & d=3 \\ 3.34\ldots & d=4 \\ 4 & d=\infty. \end{cases} \tag{117}$$

F. Multiple strips and mutual information

Our results not scaling with $\mathrm{Vol}[R]$ can be generalized to regions R consisting of n disjoint finite strips by simply applying the same argument to each connected component of the HRT surface separately. For $d = 2$ this results in

$$\left|\frac{\mathrm{d}S_R}{\mathrm{d}t}\right| \le n\sqrt{\frac{8\pi c}{3}}\langle T_{tt}\rangle. \tag{118}$$

It is easy to see that (114) also holds true for n strips. No modification is needed, since $\mathrm{Area}[\partial R]$ implicitly contains the factor of n present in the $d = 2$ case.

For the bounds scaling like volume, the behavior is different, since the upper bound depends on the connectivity properties of the entanglement wedge (EW). Consider for example $d = 2$ and the three intervals R_1, R_2, R_3 in Fig. 4, and let $R = R_1 \cup R_3$ be the region under consideration. We then see that

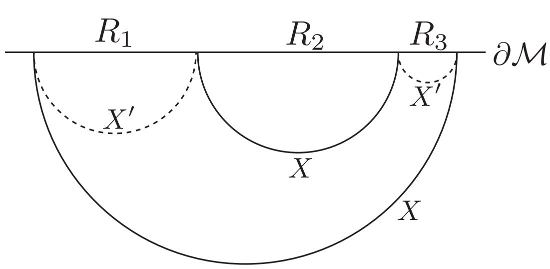

FIG. 4. Possible HRT surfaces X and X' of the region $R_1 \cup R_3$, projected onto a timeslice.

$$\left|\frac{\mathrm{d}S_R}{\mathrm{d}t}\right| \le \kappa\langle T_{tt}\rangle \begin{cases} \mathrm{Vol}[R] & \text{disconnected EW}, \\ \mathrm{Vol}[R] + 2\mathrm{Vol}[R_2] & \text{connected EW}, \end{cases} \tag{119}$$

where κ is the relevant numerical prefactor in Theorem 3. We get this result by adding the different volume factors from each connected component of the HRT surface. Similar games can be played for n strips in d dimensions.

Next, lets us consider $d = 2$ and the mutual information between two subsystems R_1 and R_2 consisting of n_1 and n_2 finite intervals, respectively. We then have

$$\begin{aligned} |\partial_t I(R_1, R_2)| &= |\partial_t S_{R_1} + \partial_t S_{R_2} - \partial_t S_{R_1R_2}| \\ &\le |\partial_t S_{R_1}| + |\partial_t S_{R_2}| + |\partial_t S_{R_1R_2}| \\ &\le (2n_1 + 2n_2)\sqrt{\frac{8\pi c}{3}}\langle T_{tt}\rangle. \end{aligned} \tag{120}$$

Using (25), the generalization to higher d is obvious.

III. MAXIMAL RATES FOR BALLS AND WILSON LOOPS

A. Setup and summary of results

In this section we will consider extremal surfaces X_t of dimension $q + 1$ anchored at q-dimensional spheres ∂R_t at time t on the conformal boundary. For $q = 0$, ∂R_t just consists of two points, and X_t is a one-parameter family of geodesics. For $q = d - 2$, X_t is a one-parameter family of HRT surfaces anchored at spheres. For $q = 1$, X_t are two-dimensional spacelike world sheets anchored at circles. The main application will be to derive growth bounds on Wilson loops and entanglement entropy for ball regions. However, we will also be able to given novel strengthenings of the positive mass theorem in odd-dimensional spacetimes.

As before we are working with planar symmetric spacetimes, subject to the same assumptions described in Sec. II A. The logical steps will be mostly identical to Sec. II, but with extra technicalities coming from the curvature of ∂R_t. Note that since we now have submanifolds of varying dimensions, we will use the symbol $\|\cdot\|$ to indicate the measure of the surface in the natural induced volume form. For quantities on the conformal boundary, $\|\cdot\|$ means with respect to the induced metric from the Minkowski conformal frame. We will use Length[], Area[] and Vol[] to refer to the measure of surfaces of dimension 1, codimension 2, and codimension 1, respectively.

To describe the relevant subregions in our results, let z be Cartesian coordinates in the direction transverse to the sphere ∂R_t. We now choose coordinates for our Minkowski conformal frame on the boundary to be

$$\mathrm{d}s^2 = -\mathrm{d}t^2 + L^2(\mathrm{d}\phi^2 + \phi^2\mathrm{d}\Omega_q^2 + \mathrm{d}z^2), \tag{121}$$

with $\mathrm{d}\Omega_q^2$ the metric of a round unit q-sphere, and with the constant–t slices the ones on which one-point functions of local operators are constant. For $q=0$ there is no $\mathrm{d}\Omega_q^2$–term, while for $q=d-2$ there is no $\mathrm{d}z^2$ term. ϕ is a dimensionless radial coordinate on the boundary, and $R_{t'}$ is given by

$$0 \le \phi \le \frac{\mathcal{R}}{L}, \qquad t=t', \qquad z=0. \tag{122}$$

We now have

$$\|\partial R_t\| = \|\partial R\| = \Omega_q \mathcal{R}^q, \tag{123}$$

where Ω_q is the volume of a unit q-sphere, and $\mathcal{R}$ the radius of R_t, which is kept constant in time.

Let us now summarize the results proven in this section. For entanglement entropy, we will prove the parts Theorems 2, 3, and 5 that refer to spherical ∂R. For extremal surfaces of more general dimensionalities, the following is our strongest theorem:

Theorem 6. Let $(\mathcal{M}, g_{ab})$ be a regular asymptotically AdS$_{d+1}$ spacetime with planar symmetry satisfying the DEC. Assume that d is even, and let be X_t be an extremal surface of dimension $d/2$, anchored on the conformal boundary at the sphere ∂R_t. Then

$$\left|\frac{\mathrm{d}}{\mathrm{d}t}\|X_t\|\right| \le \|\partial R\| L^{\frac{d}{2}} \sqrt{\frac{16\pi}{c_{\mathrm{eff}}(d-1)}\langle T_{tt}\rangle}. \tag{124}$$

Of course, for $d=2$, this just reduces to Theorem 1. For $d=4$ this can be converted to the growth bound on circular Wilson loops, given by (10) [or by (173) in terms of the effective central charge and effective 't Hooft coupling]. Making no reference to the CFT, we can also write this as a lower bound on the spacetime mass density $\mu(\infty)$: [126]

$$\mu(\infty) \ge \left(\frac{L^q}{\Omega_q \mathcal{R}^q}\frac{\mathrm{d}}{\mathrm{d}t}\|X_t\|\right)^2. \tag{125}$$

This says that rapid changes in extremal surface areas require large mass.

Next, for surfaces X_t anchored at small spheres on the boundary, we get the following:

Theorem 7. Let $(\mathcal{M}, g_{ab})$ be a regular asymptotically AdS$_{d+1}$ spacetime with planar symmetry satisfying the DEC. Let be X_t be an extremal surface of dimension $q+1$, anchored on the conformal boundary at the sphere ∂R_t having radius $\mathcal{R}$. Assume that

$$q \ge \frac{d-2}{2} \tag{126}$$

and

$$\frac{\mathcal{R}^d \langle T_{tt}\rangle}{c_{\mathrm{eff}}} \ll 1. \tag{127}$$

Then

$$\left|\frac{\mathrm{d}}{\mathrm{d}t}\|X_t\|\right| \le \eta_{d,q}\|\partial R\| L^{q+1}\mathcal{R}^{d-q-1}\frac{\langle T_{tt}\rangle}{c_{\mathrm{eff}}} \times \left[1+\mathcal{O}\left(\frac{\mathcal{R}^d\langle T_{tt}\rangle}{c_{\mathrm{eff}}}\right)\right], \tag{128}$$

where

$$\eta_{d,q} = \frac{8\pi}{d-1}\left[\frac{\Gamma\left(\frac{1}{2(q+1)}\right)}{\sqrt{\pi}\Gamma\left(\frac{q+2}{2(q+1)}\right)}\right]^{d-q-1}. \tag{129}$$

Using well known dictionary entries, described in Sec. III F, this converts to growth bounds on the entanglement of small balls and small circular Wilson loops. Specifically, for the latter, we get for $d \in \{3,4\}$ that

$$\left|\frac{\mathrm{d}}{\mathrm{d}t}\log|\langle \mathcal{W}(C)\rangle_{\rho(t)}|\right| \le \frac{8\pi\sqrt{\lambda_{\mathrm{eff}}}}{(d-1)c_{\mathrm{eff}}}\eta_{d,1}\mathcal{R}^{d-1}\langle T_{tt}\rangle + \ldots, \tag{130}$$

where $\sqrt{\lambda_{\mathrm{eff}}} = L^2/\ell_{\mathrm{string}}^2$ is the effective 't Hooft coupling, and ℓ_{string} the bulk string length. Corrections scale as $\mathcal{O}(\mathcal{R}^d\langle T_{tt}\rangle/c_{\mathrm{eff}})$.

Finally, for thin-shell spacetimes, we prove the following:

Theorem 8. Let $(\mathcal{M}, g_{ab})$ be a spacetime satisfying the same assumptions as in Theorem 2. Assume that X_t is an extremal surface anchored at a boundary sphere of dimension

$$q \ge \frac{d-2}{2}. \tag{131}$$

Then

$$\left|\frac{\mathrm{d}}{\mathrm{d}t}\|X_t\|\right| \le \|\partial R\| L^{q+1}\left[\frac{16\pi}{(d-1)c_{\mathrm{eff}}}\langle T_{tt}\rangle\right]^{\frac{q+1}{d}} \tag{132}$$

and

$$\left|\frac{\mathrm{d}}{\mathrm{d}t}\|X_t\|\right| \le \kappa_{d,q}\|\partial R\| L^{q+1}\mathcal{R}^{d-q-1}\frac{\langle T_{tt}\rangle}{c_{\mathrm{eff}}} \tag{133}$$

with $\kappa_{d,q}$ given by (192).

The main application of (132) is to bound Wilson loops in $d=3$, where we get

$$\left|\frac{\mathrm{d}}{\mathrm{d}t}\log|\langle\mathcal{W}(C)\rangle_{\rho(t)}|\right| \le \frac{\sqrt{\lambda_{\mathrm{eff}}}\mathrm{Length}[C]}{2\pi}\left[\frac{8\pi}{c_{\mathrm{eff}}}\langle T_{tt}\rangle\right]^{2/3}. \tag{134}$$

Let us now turn to the proofs.

B. An implicit solution for the extremal surface location

As earlier, let Σ be the extended planar symmetric homology hypersurface containing X. For the exact same reason as earlier, there is a unique choice of Σ. We can now pick coordinates on Σ given by

$$\mathrm{d}s^2|_\Sigma = H_{\mu\nu}\mathrm{d}y^\mu\mathrm{d}y^\nu = B(r)\mathrm{d}r^2 + r^2(\mathrm{d}\phi^2 + \phi^2\mathrm{d}\Omega_q^2 + \mathrm{d}z^2). \tag{135}$$

Again, one such coordinate system covers all of Σ, as shown in Appendix A 6.

We take our intrinsic coordinates on X to be (r, Ω^i), where Ω^i are coordinates on the sphere. The embedding coordinates of X in Σ reads

$$X^\mu = (r, \phi = \Phi(r), \Omega^i, z = 0), \tag{136}$$

where the symmetries of the problem dictate $z = 0$. The induced metric on X is

$$\mathrm{d}s^2|_X = [B(r) + r^2\Phi'(r)^2]\mathrm{d}r^2 + r^2\Phi(r)^2\mathrm{d}\Omega_q^2. \tag{137}$$

Now we must implement the condition that X is extremal, which requires us to compute all its mean curvatures and demand them to be vanishing. To do this, let n_a^I be an orthonormal basis of normal forms to X that are tangent to Σ, labeled by I. Let t_a be the future timelike normal orthogonal to Σ. A complete basis of mean curvatures of X now is

$$\begin{aligned}\mathcal{K}^I &= h^{ab}\nabla_a n_b^I,\\ \mathcal{K}^0 &= h^{ab}\nabla_a t_b,\end{aligned} \tag{138}$$

where $h^{ab} = g^{ab} + t^a t^b - \delta^{IJ} n_I^a n_J^b$. All of these quantities must vanish. Considering the $\mathcal{K}^I$ corresponding the z directions, we just get 0 by our symmetries. Letting $I = n$ denote the remaining normal direction in Σ, we get by direct computation that (see Appendix A 7)

$$\begin{aligned}\mathcal{K}^n = &\frac{1}{r\sqrt{B}[B + r^2(\Phi')^2]^{3/2}}\Big[r^2B\Phi'' + (q+1)r^3(\Phi')^3\\ &+\left((q+2)B - \frac{1}{2}rB'\right)r\Phi' - \frac{qB}{\Phi}(B + r^2(\Phi')^2)\Big].\end{aligned} \tag{139}$$

If it was not for the last term, we would reproduce (33) by setting $q = d - 2$. The new term is caused by the curvature of ∂R. Now, with this last term, we no longer have an explicit analytical solution (when $q > 0$). However, we can find an implicit solution that lets us proceed. Define

$$\chi(r) = \frac{qB}{\Phi\Phi'}\left(\frac{B}{\Phi'^2} + r^2\right), \tag{140}$$

so that our equation for extremality reads

$$\begin{aligned}&(q+1)r^3(\Phi')^3 + \left((q+2)B - \frac{1}{2}rB'\right)r\Phi'\\ &\quad + r^2B\Phi'' - (\Phi')^3\chi(r) = 0.\end{aligned} \tag{141}$$

Imposing $\Phi(r_0) = 0$, where r_0 is the tip of the extremal surface, we have the implicit solution

$$\Phi(r) = \int_{r_0}^{r}\mathrm{d}\rho\frac{\sqrt{B(\rho)}}{\rho\sqrt{\mathcal{C}\rho^{2q+2}h(\rho) - 1}}, \tag{142}$$

where

$$h(r) = 1 - \frac{2}{\mathcal{C}}\int_{r_0}^{r}\mathrm{d}\rho\chi(\rho)\rho^{-6-2q}, \tag{143}$$

for some $\mathcal{C}$ that is fixed by imposing $\Phi'(r_0) = \infty$. Assuming $h(r_0)$ is finite, we get that $\mathcal{C} = r_0^{-2q-2}$. This is indeed correct, even though $\chi(r_0)$ looks superficially divergent. Since we are near a minimum of $r(\Phi)$ we have that $r = r_0 + \mathcal{O}(\Phi^2)$ near r_0, and so for r close to r_0 we get $\Phi = \alpha\sqrt{r - r_0}$ for some α. Even though Φ goes to zero at r_0 we find that

$$\chi(r) \sim \mathcal{O}(1) \tag{144}$$

near r_0, and so $h(r_0) = 1$. Next, reality of $\Phi(r)$ demands that $h(\rho) \ge (r_0/r)^{2q+2}$, while positivity of Φ and Φ' ensures that $h(r) \le 1$, and so in total we know that [127]

$$\begin{aligned}&\Phi(r) = \int_{r_0}^{r}\mathrm{d}\rho\frac{\sqrt{B(\rho)}}{\rho\sqrt{(\rho/r_0)^{2q+2}h(\rho) - 1}},\\ &0 < (r_0/r)^{2q+2} < h(r) \le 1.\end{aligned} \tag{145}$$

C. The relation between the Hawking masses

Take $K_{\alpha\beta}$ to be the extrinsic curvature of the extended homology hypersurface. Like in the case of the strip, we have that

$$\mu(r) = \omega(r) + r^{d-4}K_{\phi\phi}(r)^2, \tag{146}$$

which follows from the same computation as in the previous section, together with (A43) in Appendix A 7. We have that $K_{\phi\phi} \sim \mathcal{O}(1/r^{q-1})$, as becomes clear in the next section. Thus, at large r we have

$$\mu(r) = \omega(r) + \mathcal{O}(r^{d-2-2q}). \tag{147}$$

Consequently, $\omega(\infty)$ is proportional to spacetime mass if and only if

$$q > \frac{d-2}{2}. \tag{148}$$

If $2q = d-2$, $\omega(\infty)$ is smaller than $\mu(\infty)$ by some finite number. For $2q < d-2$, we get $\omega(\infty) = -\infty$ by (147) and the fact that $\mu(\infty)$ is finite and positive. We will see below that this comes out of the constraint equations, since exactly when $2q < d-2$, $\omega(r)$ is neither positive nor monotonically increasing. We will not be able to say anything about the case $2q < d-2$.

D. $\partial_t \|X_t\| \leq$ momentum on X_t

The time-derivative of the generalized volume satisfies [104,107]

$$\frac{\mathrm{d}}{\mathrm{d}t}\|X_t\| = \int_{\partial X_t} N^a \eta_a, \tag{149}$$

where $\eta^a = (\partial_t)^a$ generates the deformation of ∂X_t, while N^a is the unit vector that is (1) tangent to X_t, (2) orthogonal to ∂X_t, and (3) pointing toward the conformal boundary. A computation in Appendix A 5 shows that (149) can be written as

$$\frac{\mathrm{d}}{\mathrm{d}t}\|X_t\|\|_{t=0} = -\frac{\|\partial R\|}{L^q}\lim_{r\to\infty} r^{q-1}K_{\phi\phi}(r). \tag{150}$$

Now we again reach the stage where we must write the Einstein constraint equations as a closed system, which requires us to impose extremality in the timelike direction.

First, note that from the planar symmetry of Σ, if $\boldsymbol{x}$ are Cartesian coordinates on the plane containing R, then we have that the extrinsic curvature of Σ reads

$$\begin{aligned} K_{\mu\nu}\mathrm{d}y^\mu \mathrm{d}y^\nu &= K_{rr}(r)\mathrm{d}r^2 + K_{\phi\phi}(r)(\mathrm{d}\boldsymbol{x}^2 + \mathrm{d}z^2) \\ &= K_{rr}(r)\mathrm{d}r^2 + K_{\phi\phi}(r)(\mathrm{d}\phi^2 + \phi^2\mathrm{d}\Omega_q^2 + \mathrm{d}z^2). \end{aligned} \tag{151}$$

Thus, the components of the extrinsic curvature with indices in the sphere directions reads

$$K_{ij} = K_{\phi\phi}(r)\phi^2 w_{ij}, \tag{152}$$

where w_{ij} is the unit metric on the q-sphere. Define again $F(r)$ through the relation $K_{rr}(r) = F(r)B(r)$. Computing $\mathcal{K}^0 = 0$, using (152), and solving for $F(r)$ (see Appendix A 7), we get, after substituting our expression for $\Phi(r)$, that

$$F(r) = -\frac{K_{\phi\phi}(r)}{r^2}H(r), \tag{153}$$

where we for convenience defined the function

$$H(r) = \frac{q(r/r_0)^{2q+2}h(r) + 1}{(r/r_0)^{2q+2}h(r) - 1}. \tag{154}$$

Since $\partial_h H < 0$ and $h(r) \leq 1$, we get the lower bound

$$H(r) \geq \frac{q(r/r_0)^{2q+2} + 1}{(r/r_0)^{2q+2} - 1} \equiv H_L(r). \tag{155}$$

The constraint equations (43) and (44) are unchanged, except now the expression for $F(r)$ is different. Plugging it in we get

$$(d-1)\frac{\omega'(r)}{r^{d-1}} = 2\mathcal{E} + \frac{(d-1)}{r^4}K_{\phi\phi}(r)^2[2H(r) - d + 2], \tag{156}$$

$$K'_{\phi\phi} + [H(r) - 1]\frac{K_{\phi\phi}}{r} = -\frac{r^2}{d-1}\mathcal{J}(r). \tag{157}$$

Now, using the lower bound $H_L(r)$, let us note the following:

$$2H(r) - d + 2 \geq \frac{(2q-d+2)(r/r_0)^{2q+2} + d - 1}{(r/r_0)^{2q+2} - 1}. \tag{158}$$

This is positive definite for all r only when $q \geq \frac{d-2}{2}$, so for geodesics ($q = 0$), we only have monotonicity of $\omega(r)$ when $d = 2$. But this is just the case studied in the previous section. For ($q = 1$), which is the relevant case for Wilson loops, we have monotonicity of $\omega(r)$ only for $d \leq 4$. For an HRT surface we have $q = d-2$, and so we have monotonicity in all dimensions. It is in fact quite surprising that we have monotonicity for any q whatsoever, since when looking at the Einstein constraint equations in covariant form, monotonicity of the Riemannian Hawking mass is only manifest on hypersurfaces that have vanishing mean curvature.

Let us assume $2q \geq d-2$ going forward, and let us bound $K_{\phi\phi}$ and μ at infinity. Fixing an integration constant by demanding that $F(r_0) =$ finite, the solution to the momentum constraint is

$$K_{\phi\phi}(r) = -\frac{1}{d-1}\int_{r_0}^{r}\mathrm{d}\rho\rho^2\mathcal{J}(\rho)e^{-\int_\rho^r \mathrm{d}z\frac{1}{z}(H(z)-1)}. \tag{159}$$

We have that

$$|K_{\phi\phi}(r)| \leq \frac{1}{d-1}\int_{r_0}^{r} \mathrm{d}\rho\rho^2|\mathcal{J}(\rho)|e^{-\int_\rho^r \mathrm{d}z\frac{1}{z}(H_L(z)-1)}$$
$$= \frac{r^2}{(d-1)\sqrt{(r/r_0)^{2q+2}-1}}$$
$$\int_{r_0}^{r}\mathrm{d}\rho|\mathcal{J}(\rho)|\sqrt{(\rho/r_0)^{2q+2}-1}. \tag{160}$$

We see from this expression that $K_{\phi\phi} \sim \mathcal{O}(1/r^{q-1})$. Also, in this last expression, if we replace $|\mathcal{J}| \to -\mathcal{J}$, we just get the solution of (157) with $H(r)$ replaced by $H_L(r)$. We will use this fact later.

Inserting (160) in (150), we finally get

$$\left|\frac{\mathrm{d}}{\mathrm{d}t}\|X_t\|\right| \leq \frac{(d-1)\|\partial R\|}{L^q}\int_{r_0}^{\infty}\mathrm{d}\rho|\mathcal{J}(\rho)|\sqrt{\rho^{2q+2}-r_0^{2q+2}}. \tag{161}$$

Unlike for an HRT surface anchored at a strip, we are here only able to write an inequality.

Next, let us turn to the second ingredient: the mass. Rewriting (156) in terms of $\mu(r)$, we get

$$(d-1)\frac{\mu'(r)}{r^{d-1}} = 2\mathcal{E} + \frac{(d-1)}{r^4}K_{\phi\phi}(r)^2[2H(r)+d-6] + \frac{2(d-1)}{r^3}\frac{\mathrm{d}}{\mathrm{d}r}K_{\phi\phi}^2. \tag{162}$$

After an integration by parts and using $H(r) \geq H_L(r)$, we get that

$$\mu(\infty) \geq \mu(r_0) + \frac{2}{d-1}\int_{r_0}^{\infty}\mathrm{d}\rho\rho^{d-1}\mathcal{E}(\rho) + \int_{r_0}^{\infty}\mathrm{d}\rho\rho^{d-5}K_{\phi\phi}(r)^2[2H_L(r)+d], \tag{163}$$

where

$$2H_L(r)+d = \frac{(d+2q)(r/r_0)^{2q+2}+(d-2)}{(r/r_0)^{2q+2}-1} \geq 0. \tag{164}$$

Possessing now an upper bound on $\partial_t\|X_t\|$ and a lower bound on mass, we next need an upper bound on L^2/r_0.

E. Constraints on boundary anchored extremal surfaces

It turns out that generalizations of Lemmata 2 and 3 remain true for the surfaces considered in this section. The proof of Lemma 2 is unchanged, while from the discussion in Appendixes A 6 and A 7, together with the proof of Lemma 3, we get the following constraints on the tip of X:

Lemma 5. Let $(\mathcal{M}, g_{ab})$ be an asymptotically $\mathrm{AdS}_{d+1\geq 3}$ spacetime with planar symmetry. Let X be a $(q+1)$-dimensional extremal surface anchored at a q-sphere on the conformal boundary. Then the tip of X lies in an untrapped region. Furthermore, if $(\mathcal{M}, g_{ab})$ is regular and satisfies the DEC, then $\omega(r_0) \geq 0$, where r_0 is the radius of the tip of X.

With this in hand, we readily obtain the spherical dimension–$(q+1)$ version of Theorem 4:

Theorem 9. Let $(\mathcal{M}, g_{ab})$ be a regular planar-symmetric asymptotically $\mathrm{AdS}_{d+1\geq 3}$ spacetime satisfying the DEC. Let X be a dimension $q+1$ extremal surface anchored at a sphere of radius $\mathcal{R}$. Let be r_0 be the radius of the plane tangent to the tip of X. Then if

$$q \geq \frac{d-2}{2}, \tag{165}$$

we have

$$\frac{L^2}{r_0} \leq \frac{\Gamma\left(\frac{1}{2(q+1)}\right)}{\sqrt{\pi}\Gamma\left(\frac{q+2}{2(q+1)}\right)}\mathcal{R}. \tag{166}$$

Proof. For $2q \geq d-2$, (156) implies $\omega'(r) \geq 0$. Combining with $\omega(r_0) \geq 0$, we get $\omega(r) \geq 0$. Using now $h(r) < 1$ and that $\omega(r) \geq 0$ implies $B(r) \geq L/r$, we get

$$\mathcal{R} = L\Phi(\infty) = L\int_{r_0}^{\infty}\mathrm{d}r\frac{\sqrt{B(r)}}{r\sqrt{(r/r_0)^{2q+2}h(r)-1}}$$
$$\geq L^2\int_{r_0}^{\infty}\mathrm{d}r\frac{1}{r^2\sqrt{(r/r_0)^{2q+2}-1}}$$
$$= \frac{L^2}{r_0}\frac{\sqrt{\pi}\Gamma\left(\frac{q+2}{2(q+1)}\right)}{\Gamma\left(\frac{1}{2(q+1)}\right)}. \tag{167}$$

■

F. Proofs

1. Bounds for even d

Consider the special dimension

$$q = \frac{d-2}{2}, \tag{168}$$

which can only happen when d is even. As seen previously, we have that $\omega(r) \geq 0$ in this case. Furthermore, (146) becomes

$$\mu(\infty) = \omega(\infty) + [\lim_{r\to\infty} r^{q-1}K_{\phi\phi}]^2, \tag{169}$$

and so

$$|\lim_{r\to\infty} r^{q-1}K_{\phi\phi}(\infty)| \leq \sqrt{\mu(\infty)}, \tag{170}$$

which gives

$$\left|\frac{\mathrm{d}}{\mathrm{d}t}\|X_t\|\right|_{t=0} \leq \frac{\|\partial R\|}{L^q}\sqrt{\mu(\infty)}$$
$$= \|\partial R\| L^{q+1}\sqrt{\frac{16\pi}{c_{\mathrm{eff}}(d-1)}\langle T_{tt}\rangle}. \tag{171}$$

This proves Theorem 6.

Next, for $d=4$, (171) holds for $q=1$, where the X_t are two-dimensional world sheets anchored at circles on the boundary. If $\mathcal{W}(C)$ is a Wilson loop of a circle $C=S^1$, we have that [128,129]

$$\langle\mathcal{W}(C)\rangle_{\rho(t)} = \eta e^{-\frac{1}{2\pi\alpha'}\|X_t\|}, \tag{172}$$

where $\alpha' = \ell_{\mathrm{string}}^2$ and η again some constant. Combining (171) and (172) we get

$$\left|\frac{\mathrm{d}}{\mathrm{d}t}\log\langle\mathcal{W}(C)\rangle_{\rho(t)}\right| \leq \mathrm{Length}[C]\sqrt{\frac{4\lambda_{\mathrm{eff}}}{3\pi c_{\mathrm{eff}}}\langle T_{tt}\rangle}, \tag{173}$$

where $\mathrm{Length}[C]=2\pi\mathcal{R}$. With the precise dictionary for the duality between type IIB supergravity on $\mathrm{AdS}_5\times S^5$ and $\mathcal{N}=4$ super Yang-Mills with gauge group $SU(N)$ and 't Hooft coupling λ, given by

$$\frac{G_N}{R^3} = \frac{\pi}{2N^2}, \qquad \sqrt{\lambda} = \frac{L^2}{\alpha'}, \tag{174}$$

(173) can be written as (10).

2. Proof of bounds for small $\mathcal{R}$

Next we prove bounds that are strong at small radii $\mathcal{R}$. We have:

Lemma 6. Consider the same assumptions as in Theorem 9. Assume furthermore that $\mathcal{R}^d\langle T_{tt}\rangle/c_{\mathrm{eff}} \ll 1$ and $2q \geq d-2$. Then

$$|\lim_{r\to\infty} r^{d-3}K_{\phi\phi}| \leq \frac{L}{2r_0^{d-q-1}}\omega(\infty)\left[1+\mathcal{O}\left(\frac{\mathcal{R}^d\langle T_{tt}\rangle}{c_{\mathrm{eff}}}\right)\right]. \tag{175}$$

Proof. Define $W = -\lim_{r\to\infty} r^{q-1}K_{\phi\phi}$, and assume without loss of generality that $W>0$. Using (55) and (156) and the exact same logic as in the proof of Lemma 4, we get

$$\frac{W}{\omega(\infty)} \leq \frac{L\int_{r_0}^{\infty}\mathrm{d}r r^{q+1}|\mathcal{J}(r)|}{2\int_{r_0}^{\infty}\mathrm{d}r r^d\sqrt{1-\frac{\omega(r)L^2}{r^d}}|\mathcal{J}(r)|}$$
$$\leq \frac{L\int_{r_0}^{\infty}\mathrm{d}r r^{q+1}|\mathcal{J}(r)|}{2\int_{r_0}^{\infty}\mathrm{d}r r^d|\mathcal{J}(r)|}\left[1+\frac{L^2\omega(\infty)}{2r_0^d}+\ldots\right]$$
$$\leq \frac{L}{2r_0^{d-q-1}}\left[1+\mathcal{O}\left(\frac{\mathcal{R}^d\langle T_{tt}\rangle}{c_{\mathrm{eff}}}\right)\right]. \tag{176}$$

■

Inserting now (175) into (150), we get

$$\left|\frac{\mathrm{d}}{\mathrm{d}t}\|X_t\|\right|_{t=0} \leq \frac{8\pi\|\partial R\|L^{1+q}}{(d-1)c_{\mathrm{eff}}}\frac{L^{2(d-q-1)}}{r_0^{d-q-1}}\langle T_{tt}\rangle$$
$$\leq \frac{\|\partial R\|L^{1+q}}{c_{\mathrm{eff}}}\eta_{d,q}\mathcal{R}^{d-q-1}\langle T_{tt}\rangle, \tag{177}$$

where

$$\eta_{d,q} = \frac{8\pi}{d-1}\left[\frac{\Gamma\left(\frac{1}{2(q+1)}\right)}{\sqrt{\pi}\Gamma\left(\frac{q+2}{2(q+1)}\right)}\right]^{d-q-1}. \tag{178}$$

We can convert this to bounds on two-point functions and circular Wilson loops. Combining (177) with (82) and (172), we get the bounds (92) and (130).

Finally, with $q=d-2$ and $d>2$, the entanglement entropy of small spheres is bounded as

$$\left|\frac{\mathrm{d}S_R}{\mathrm{d}t}\right| \leq \frac{2\sqrt{\pi}\Gamma\left(\frac{1}{2(d-1)}\right)}{\Gamma\left(\frac{d}{2(d-1)}\right)}\mathrm{Vol}[R]\langle T_{tt}\rangle + \ldots \tag{179}$$

where we used that $\mathrm{Vol}[R] = \mathrm{Area}[\partial R]\mathcal{R}/(d-1)$. This proves the part of Theorem 3 where ∂R is a sphere.

3. Proof of bounds for thin-shell spacetimes

Finally, let us prove our thin-shell results, assuming $2q \geq d-2$. Since we already have general bounds on Wilson loops in $d=4$ and balls for small $\mathcal{R}$, this section is most relevant for entanglement in medium or large balls in general d, and for Wilson loops in $d=3$. We consider the same setup as in Sec. II E, and use the same notation. Again, we choose $r_0=L=1$.

Now, let us consider the solutions (156) and (157) with the replacement $H(r)\to H_L(r)$. As discussed in Sec. III D, this gives a smaller value for $\mu(\infty)$ and larger value for $|\lim r^{q-1}K_{\phi\phi}|$ if $\mathcal{J}$ has a fixed sign, which is the case here. Since we will consider bounds of the form $\lim r^{q-1}K_{\phi\phi} \leq \#\mu(\infty)^n$ for $n>0$, the bounds we obtain with this replacement will be valid for the original spacetime.

Now, with a delta function shock, solution for $K_{\phi\phi}$ reads

$$K_{\phi\phi}(r) = -\frac{r^2}{d-1}\eta\sqrt{\frac{\hat{r}^{2q+2}-1}{r^{2q+2}-1}}\theta(r-\hat{r}) = -\frac{r^2 W}{\sqrt{r^{2q+2}-1}}\theta(r-\hat{r}). \quad (180)$$

From (163) we get that the contribution to $\mu(\infty)$ from the extrinsic curvature reads

$$Q(\infty) \equiv \int_{r_0}^{\infty} \mathrm{d}\rho\rho^{d-5}K_{\phi\phi}(r)^2\frac{(d+2q)r^{2q+2}+(d-2)}{r^{2q+2}-1} = W^2\frac{\hat{r}^d}{\hat{r}^{2q+2}-1}. \quad (181)$$

The analysis of how the DEC changes across the shock is unchanged from the strip case, except for a few exponents, and we find

$$\omega_+ = \omega_- + \frac{\hat{r}^d}{\sqrt{\hat{r}^{2q+2}-1}}W\left[\sqrt{1-\frac{\omega_-}{\hat{r}^d}} - \frac{W}{\sqrt{\hat{r}^{2q+2}-1}}\right]. \quad (182)$$

By the same logic as in Sec. II E we get,

$$\frac{W^n}{\mu(\infty)} \leq \frac{W^n}{\omega_- + W\frac{\hat{r}^d}{\sqrt{\hat{r}^{2q+2}-1}}\sqrt{1-\frac{\omega_-}{\hat{r}^d}}} \equiv U_n, \quad (183)$$

where

$$0 \leq \omega_- \leq \hat{r}^d, \quad (184)$$

$$W \leq \sqrt{r^{2q+2}-1}\sqrt{1-\frac{\omega_-}{\hat{r}^d}}. \quad (185)$$

Again, it now suffices to take ω_- at the boundary of its allowed domain. With $\omega_- = 0$ and $1 \leq n \leq \frac{d}{q+1}$ we get

$$U_n = \frac{W^{n-1}\sqrt{\hat{r}^{2q-2}-1}}{\hat{r}^d} \leq \frac{[r^{2q+2}-1]^{n/2}}{\hat{r}^d} \leq 1, \quad (186)$$

and for $n = 1$ we get the stronger bound

$$U_1 \leq \sqrt{\frac{q+1}{d}}\left(\frac{d}{d-1-q}\right)^{\frac{q+1-d}{2(q+1)}} \equiv \alpha_{d,q}. \quad (187)$$

For saturation of (185), neglecting the first ω_- in the denominator of U_n and using that $W \leq \sqrt{\hat{r}^{2q+q}-1}$, we get

$$U_n \leq \frac{[r^{2q+2}-1]^{n/2}}{\hat{r}^d} \leq 1. \quad (188)$$

Restoring factors of L, r_0, we have the following general bounds

$$W \leq \alpha_{q,d}\frac{L}{r_0^{d-q-1}}\omega(\infty), \quad (189)$$

$$W \leq L^{\frac{2q+2-d}{d}}\omega(\infty)^{\frac{q+1}{d}}. \quad (190)$$

Combining (189) with (150) and (165) now gives that

$$\left|\frac{\mathrm{d}}{\mathrm{d}t}\|X_t\|\right| \leq \kappa_{d,q}\|\partial R\|L^{1+q}\mathcal{R}^{d-q-1}\frac{\langle T_{tt}\rangle}{c_{\mathrm{eff}}}, \quad (191)$$

where

$$\kappa_{d,q} = \frac{16\pi}{d-1}\sqrt{\frac{q+1}{d}}\left(\frac{d}{d-1-q}\right)^{\frac{q+1-d}{2(q+1)}} \times \left[\frac{\Gamma\left(\frac{1}{2(q+1)}\right)}{\sqrt{\pi}\Gamma\left(\frac{q+2}{2(q+1)}\right)}\right]^{d-q-1}. \quad (192)$$

This shows that the type of bounds derived in the small $\mathcal{R}$ limit holds in thin shell spacetimes for all $\mathcal{R}$, at price of a larger prefactor. For the entanglement entropy of balls, we get

$$\left|\frac{\mathrm{d}S_R}{\mathrm{d}t}\right| \leq 4\sqrt{\frac{\pi(d-1)}{d^{\frac{d}{d-1}}}}\frac{\Gamma\left(\frac{1}{2(d-1)}\right)}{\Gamma\left(\frac{d}{2(d-1)}\right)}\mathrm{Vol}[R]\langle T_{tt}\rangle. \quad (193)$$

For Wilson loops we get

$$\left|\frac{\mathrm{d}}{\mathrm{d}t}\log|\langle\mathcal{W}(C)\rangle_{\rho(t)}|\right| \leq f_d\frac{\sqrt{\lambda_{\mathrm{eff}}}}{c_{\mathrm{eff}}}\mathcal{R}^{d-1}\langle T_{tt}\rangle, \quad (194)$$

where

$$f_d = \begin{cases} \frac{\sqrt{128\pi}\Gamma(1/4)}{3^{3/4}\Gamma(3/4)} \approx 26 & d=3 \\ \frac{8\Gamma(1/4)^2}{3\Gamma(3/4)^2} \approx 23 & d=4. \end{cases} \quad (195)$$

Next, consider (190). This gives us that

$$\left|\frac{\mathrm{d}}{\mathrm{d}t}\|X_t\|\right|_{t=0} \leq \|\partial R\|L^{q+1}\left[\frac{16\pi}{(d-1)c_{\mathrm{eff}}}\langle T_{tt}\rangle\right]^{\frac{q+1}{d}} \quad (196)$$

For $q = d-2$, corresponding to entanglement for ball subregions, this just gives (25), verifying that it holds for spheres as well, completing the proof of the part of Theorem 5 concerning spherical ∂R.

For $q = 0$, $d = 2$ and $q = 1$, $d = 4$ we just reproduce the bounds of Sec. III F, which are anyway proven with weaker assumptions there. For $q = 1$, $d = 3$ we get a new bound on Wilson loops, given by (134).

IV. BOUNDING SPATIAL DERIVATIVES

The technology we have developed to bound time derivatives also lets us bound spatial derivatives of extremal surface areas for strips.

Consider a one parameter family of strips R_ℓ of variable width ℓ at some fixed boundary time, given by (18) with t' now held fixed. Let X_ℓ be the corresponding one-parameter family of HRT surfaces. A computation in Appendix A 4 gives that

$$\frac{\mathrm{d}}{\mathrm{d}\ell}\mathrm{Area}[X_\ell] = \frac{\mathrm{Area}[\partial R]}{L^{d-1}} r_0^{d-1}. \tag{197}$$

For a strip, we thus see that the radius of the HRT surface tip uniquely determines $\partial_\ell S$. To our knowledge, this is a new direction relation between entropy derivatives and geometry.

Using our lower bound on r_0 given by (61), we now immediately get the following:

Theorem 10. Let $(\mathcal{M}, g_{ab})$ be a regular asymptotically $\mathrm{AdS}_{d+1\geq 3}$ spacetime with planar symmetry satisfying the DEC. If X_ℓ is the HRT surface of a strip R_ℓ of width ℓ, then

$$\frac{\mathrm{d}}{\mathrm{d}\ell}\left[\frac{\mathrm{Area}[X_\ell]}{4G_N}\right] \geq \frac{c_{\mathrm{eff}}}{4\ell^{d-1}}\mathrm{Area}[\partial R]\left[\frac{2\sqrt{\pi}\Gamma\left(\frac{d}{2(d-1)}\right)}{\Gamma\left(\frac{1}{2(d-1)}\right)}\right]^{d-1} \tag{198}$$

The lower bound is equal to $\partial_\ell S_{\mathrm{vacuum}}$, and so we get

$$\frac{\mathrm{d}}{\mathrm{d}\ell}\Delta S[\rho_{R_\ell}] \geq 0, \tag{199}$$

where ΔS is the vacuum subtracted entropy. Since we get the vacuum entanglement entropy in the limit $\ell \to 0$, this implies that

$$\Delta S \geq 0. \tag{200}$$

It is easy to see that (199) and (200) applies to a subregion R corresponding to a union of any number of finite width strips, with ∂_ℓ now interpreted as the derivative with respect to increasing width of one or more of the connected components.

For $d = 2$, we also get a bound on correlators of heavy scalar single trace primaries. Working at a fixed moment of time with a homogeneous state ρ, the combination of (61), (82), and (197) for $x > 0$ gives

$$\frac{\mathrm{d}}{\mathrm{d}x}\ln\langle\mathcal{O}(x)\mathcal{O}(0)\rangle_\rho \leq \frac{\mathrm{d}}{\mathrm{d}x}\ln\langle\mathcal{O}(x)\mathcal{O}(0)\rangle_{\mathrm{vacuum}} = -\frac{2\Delta}{x} \tag{201}$$

which means that correlations must die of faster than the vacuum for the states and operators covered by our assumptions. This in particular implies that

$$\langle\mathcal{O}(x)\mathcal{O}(0)\rangle_\rho \leq \langle\mathcal{O}(x)\mathcal{O}(0)\rangle_{\mathrm{vacuum}}, \tag{202}$$

since we just get the vacuum correlator as $x \to 0$.

V. EVIDENCE FOR BROADER VALIDITY OF BOUNDS

In the previous sections, we have shown that the DEC allows us to prove several general bounds on the growth of entanglement, correlators and Wilson loops. However, the proofs crucially relied on the dominant energy condition. While the dominant energy condition holds in type IIA, IIB and eleven-dimensional supergravity when the compact dimensions are included (see for example the Appendix of [130]), it is typically violated after dimensional reduction [131]. The prototypical example is a scalar field dual to a relevant CFT operator. This field has negative mass squared, leading to DEC violation.

Even though our proofs assumed the DEC, we will now provide strong evidence for a subset of the bounds that they hold when the DEC is violated in reasonable ways. That is, we provide evidence in scalar theories that violate the DEC, but which have proven positive mass theorems [132,133] (so pure AdS is stable) and respect the null energy condition (NEC). This is evidence that our bounds are true even in CFTs with DEC-violating bulks, since the NEC and a stable vacuum are both necessary conditions for sensible bulk theories [134].

In fact, we provide evidence not just that

$$\mathfrak{R} \leq 1, \tag{203}$$

but also that when $d > 2$,

$$\mathfrak{R} \leq v_E^{(\mathrm{SAdS})} + \delta v_E < 1 \tag{204}$$

for some small δv_E that seems to depend on the scalar potential. Here

$$v_E^{(\mathrm{SAdS})} = \sqrt{\frac{d}{d-2}}\left(\frac{d-2}{2(d-1)}\right)^{\frac{d-1}{d}} \leq 1 \tag{205}$$

is the entanglement velocity computed from a holographic quench, with the final state being neutral and dual to the AdS-Schwarzschild black brane [33,34].

The theories we will consider are neutral scalars minimally coupled to gravity,

$$8\pi G_N\mathcal{L} = \frac{1}{2}R - \frac{d(d-1)}{2L^2} - \frac{1}{2}|\mathrm{d}\phi|^2 - V(\phi), \tag{206}$$

where V is negative somewhere, leading to violation of the DEC (but not the NEC). These theories are common in consistent truncations and dimensional reductions of type IIA, IIB, and eleven-dimensional supergravity [135–138]. We consider these theories because, for standard forms of minimally coupled bosonic matter, neutral scalars appear to pose the biggest risk to our bounds. This is because gauge fields give no direct contribution to $\mathcal{J}$, and they have a manifestly positive contributions to the mass (they respect the DEC).

For free theories where $V = \frac{1}{2}m^2\phi^2$, in order to maximize the chance of violating our bounds, we choose potentials that are close to "maximally negative," meaning we pick m^2 just slightly above the Breitenlohner-Freedman [139,140] bound:

$$m^2L^2 \geq m_{\mathrm{BF}}^2 L^2 \equiv -(d/2)^2. \tag{207}$$

It is known that if $m^2 < m_{\mathrm{BF}}^2$, AdS is unstable, and so these theories cannot be dual to CFTs with a Hamiltonian that is bounded from below. Additionally, to have an example of an interacting potential, in $d = 3$ we consider a top down potential that becomes exponentially negative for large $|\phi|$. The more negative the potential, the more danger for our theorems, so this should give a fairly strong test.

A. The numerical procedure

Let us now explain our procedure. For a given $V(\phi)$ and spacetime dimension, we will construct an n-parameter family of initial data, parametrized by coefficients $\{f_i\}_{i=1}^n$. The data will be provided on an extended homology hypersurface of some HRT surface. Then we will define the function $\mathcal{A}(\{f_i\})$ to be equal to the ratio

$$|\lim_{r\to\infty} r^{d-3}K_{\phi\phi}|/\mu(\infty)^{\frac{d-1}{d}} \tag{208}$$

in the initial dataset specified by parameters $\{f_i\}$. Different initial datasets correspond to different moments of time in different spacetimes (with different sizes of R). The value of $\mathcal{A}$ in some particular initial dataset corresponds to the instantaneous value of $\mathfrak{R}$ in that configuration, and we will do a numerical maximization of $\mathcal{A}$ with respect to the parameters $\{f_i\}$. If we find that $\mathcal{A}$ is upper bounded, and that the upper bound is $\mathcal{A}_{\max}$, we have provided evidence that

$$\left|\frac{\mathrm{d}S_R}{\mathrm{d}t}\right| \leq \frac{1}{4}\mathcal{A}_{\max}\mathrm{Area}[\partial R]c_{\mathrm{eff}}\left[\frac{16\pi}{(d-1)c_{\mathrm{eff}}}\langle T_{tt}\rangle\right]^{\frac{d-1}{d}}. \tag{209}$$

If $\mathcal{A}$ is not upper bounded, or if $\mathcal{A}_{\max} > 1$, we have a counterexample to $\mathfrak{R} \leq 1$ in the theory under consideration.

We will also evaluate the function $\mathcal{B}(\{f_i\})$, which we define as the value of

$$\frac{|\partial_t S_R|}{\mathrm{Vol}[R]\langle T_{tt}\rangle} = \frac{4\pi}{d-1}\frac{L}{\ell}\frac{|\lim r^{d-3}K_{\phi\phi}|}{\mu(\infty)}\begin{cases} 2 & d=2 \\ 1 & d>2 \end{cases} \tag{210}$$

for any given initial dataset. By the same logic as earlier, if $\mathcal{B}$ is upper bounded by $\mathcal{B}_{\max}$, we have evidence that

$$\left|\frac{\mathrm{d}}{\mathrm{d}t}S[\rho_R(t)]\right| \leq \mathcal{B}_{\max}\mathrm{Vol}[R]\langle T_{tt}\rangle. \tag{211}$$

If $\mathcal{B}$ is not upper bounded, then our volume-type bounds break without the DEC.

Assuming we work with strips R, for a single evaluation of $\mathcal{A}$ and $\mathcal{B}$, we need to numerically solve the ODEs given by (51) and (52). For simplicity we will restrict to strips, since for spheres we cannot solve for $\Phi(r)$ analytically. In this case we would need to solve a set of three coupled equations instead.

Let us now specify our family of initial data. An explicit computation gives that

$$\begin{aligned} \mathcal{E} &= \frac{1}{2}\dot{\phi}(r)^2 + \frac{1}{2}\left(\frac{r^2}{L^2} - \frac{\omega(r)}{r^{d-2}}\right)\phi'(r)^2 + V(\phi), \\ \mathcal{J} &= \dot{\phi}(r)\phi(r), \end{aligned} \tag{212}$$

where $\dot{\phi} = t^a\nabla_a\phi|_\Sigma$. Specifying an initial dataset now corresponds to specifying the two profiles $\phi(r)$ and $\dot{\phi}(r)$, together with the initial value of $\omega(r_0)$. Letting

$$\Delta = d/2 + \sqrt{(d/2)^2 + m^2L^2} \tag{213}$$

be the scaling dimension of the CFT operator dual O to ϕ, the profiles we consider are

$$\begin{aligned} \phi &= f_1 \exp\left[-\left(\frac{r-f_2}{f_3}\right)^2\right] + \frac{f_4}{r^\Delta} + \frac{f_5}{r^{\Delta+2}} \\ \dot{\phi} &= f_6 \exp\left[-\left(\frac{r-f_7}{f_8}\right)^2\right] + \frac{f_9}{r^{\Delta+1}} + \frac{f_{10}}{r^{\Delta+3}} \end{aligned} \tag{214}$$

which gives a ten-parameter family of initial data. The Gaussians give localized lumps of matter, while the power law falloffs ensures that we can turn on a VEV of O in the CFT, with $\langle O\rangle \propto f_4$ and $\langle \partial_t O\rangle \propto f_8$. Note that the seemingly unusual $1/r^{\Delta+1}$ falloff in $\dot{\phi}$ is just caused by the fact that the time derivative is with respect to a unit normal rather than the more standard global time coordinate near the conformal boundary.

What remains is to pick $\omega(r_0)$. To minimize the CFT energy, we want $\omega(r_0)$ small. When the DEC holds, we know that AdS hyperbolicity implies that $\omega(r_0) \geq 0$, as proven in Lemma 3. However, without the DEC we can have that $\omega(r_0)$ is negative, but not arbitrarily negative. If we pick $\omega(r_0)$ too negative, it will forbid an embedding of Σ in a complete slice. A difficulty is that how negative $\omega(r_0)$ can be depends on $\phi(r_0)$, $\dot{\phi}(r_0)$, and $V(\phi)$. We will thus restrict to $\omega(r_0) = 0$ and relegate a more complete study of the future. Even with $\omega(r_0) = 0$, it is far from obvious if our results survive breaking of the DEC, as we can easily obtain large regions of $\omega < 0$ even with $\omega(r_0) = 0$.

Finally, we need to deal with invalid datasets. For a given scalar profile, it could be that $\omega(r)$ overshoots r^d/L^2. In this case, the relevant solution does not correspond to a spacelike hypersurface, and so it must be discarded. In this case we conventionally define $\mathcal{A} = \mathcal{B} = 0$. Consequently, the functions we are maximizing will have discontinuities.

We are now ready to proceed to the numerical results.

B. Numerical results: $d = 2$

We now consider a free massive scalar field with mass

$$m^2L^2 = 0.9m_{\mathrm{BF}}^2L^2 = -0.9, \tag{215}$$

dual to a relevant operator with $\Delta \approx 1.32$. We do not consider saturation of the BF bound, since this requires modification of the mass formula. Furthermore, we do not want to go too close to the BF bound, since then $\omega(r)$ converges slowly at large r, and so the numerical maximization procedure becomes prohibitively expensive.

Using *Mathematica*'s built in `NMaximize` function to maximize over our ten-parameter family of initial data, trying all methods for nonconvex optimization implemented in *Mathematica* and picking the best result, we find that

$$\mathcal{A}_{\max} \approx 0.999 \leq v_E|_{d=2} = 1. \tag{216}$$

Thus, in $d = 2$ we have evidence that (22) holds without the DEC—at least in free tachyonic scalar theories.

Next, maximizing $\mathcal{B}$, we find that

$$\mathcal{B}_{\max} \approx 3.29 \leq \kappa_{d=2} = 2\pi. \tag{217}$$

This provides evidence that (115) holds when the DEC is violated, and that the $\mathcal{O}(\ell^d \langle T_{tt} \rangle / c_{\mathrm{eff}})$ corrections are not needed, even though we could not prove their absence outside thin shell spacetimes. In fact, given the large gap between $\mathcal{B}_{\max}$ and $\kappa_{d=2}$, the numerical results suggest that our proofs might possibly be sharpened.

C. Numerical results: $d = 3$

Now we consider two potentials:

$$\begin{aligned} V_{\mathrm{I}}(\phi) &= \frac{1}{2}(0.9m_{\mathrm{BF}}^2)\phi^2, \\ V_{\mathrm{II}}(\phi) &= 1 - \cosh\sqrt{2}\phi, \end{aligned} \tag{218}$$

with ϕ dual to operators with scaling dimensions $\Delta_{\mathrm{I}} \approx 1.97$ and $\Delta_{\mathrm{II}} = 2$, respectively. The potential V_{II} comes from a consistent truncation and dimensional reduction of eleven-dimensional SUGRA on $\mathrm{AdS}_4 \times S^7$ [135]. We find

$$\begin{aligned} \mathcal{A}_{I,\max} &\approx 0.693, \\ \mathcal{A}_{\mathrm{II},\max} &\approx 0.702. \end{aligned} \tag{219}$$

In both cases $\mathcal{A}_{\max} < 1$, and so we have evidence that the conjectured bound (25) is true—even without the DEC and outside thin-shell spacetimes.

Now, we have that

$$v_E^{(\mathrm{SAdS})} = \frac{\sqrt{3}}{2^{4/3}} = 0.687\ldots$$

In both cases $\mathcal{A}_{\max}$ is close to $v_E^{(\mathrm{SAdS})}$, although it is slightly larger. It seems possible that a stronger bound

$$\mathfrak{R} \leq v_E^{(\mathrm{SAdS})} + \delta v_E \tag{220}$$

is true for some small δv_E that potentially depends on the scalar potential.

For $\mathcal{B}$ we find

$$\begin{aligned} \mathcal{B}_{I,\max} &\approx 1.71 \leq \kappa_{d=3} \approx 2.62, \\ \mathcal{B}_{\mathrm{II},\max} &\approx 1.72. \end{aligned} \tag{221}$$

Again, there is a significant gap, with the implications being the same as for $d = 2$.

D. Numerical results: $d = 4$

We now consider

$$V(\phi) = \frac{1}{2}(0.9m_{\mathrm{BF}}^2)\phi^2. \tag{222}$$

and find

$$\mathcal{A}_{\max} \approx 0.643. \tag{223}$$

Again we find evidence that (9) is true without the DEC or outside thin-shell spacetimes. We have

$$v_E^{(\mathrm{SAdS})} = \frac{\sqrt{2}}{3^{3/4}} = 0.620\ldots, \tag{224}$$

and so the instantaneous growth can be above $v_E^{(\mathrm{SAdS})}$, but possibly only slightly so.

We also find

$$\mathcal{B}_{\max} = 1.91 \leq \kappa_{d=4} \approx 2.43. \tag{225}$$

Again, there is a significant gap, with the implications being the same as for $d = 2$.

TABLE I. Proven bounds on entanglement, spatial Wilson loops and equal-time correlators. We suppress $O(1)$ numerical constants in the table. Dots mean corrections scaling as $\mathcal{O}(\ell^d\langle T_{tt}\rangle/c)$ where ℓ is the relevant characteristic length scale, corresponding to strip width or ball radius. We abbreviate the effective central charge and 't Hooft coupling as c and λ, respectively. For proof validity equal to quench+, we mean proofs valid for states dual to spacetimes with thin-shell matter, which includes quenches as a subset. With "general," we mean proofs valid for general regular asymptotically $\mathrm{AdS}_{d+1\geq 3}$ planar symmetric spacetime satisfying the DEC.

$\partial_t S \leq$	d	Region R	Proof validity	Equations
$\sqrt{\langle T_{tt}\rangle/c}$	2	n intervals	General	(22)
$\mathrm{Vol}[R]\langle T_{tt}\rangle+\cdots$	≥ 2	Small strip or ball	General	(28)
$\mathrm{Area}[\partial R][\langle T_{tt}\rangle/c]^{(d-1)/d}$	≥ 2	n strips	Quench+	(25)
$\mathrm{Area}[\partial R][\langle T_{tt}\rangle/c]^{(d-1)/d}$	≥ 2	Ball	Quench+	(25)
$\mathrm{Vol}[R]\langle T_{tt}\rangle$	≥ 2	Strip or ball	Quench+	(115)
$\partial_\ell S \geq$				
$\partial_\ell S_{\mathrm{vacuum}}$	≥ 2	n strips	General	(198)
$\partial_t \ln\langle \mathcal{W}(C)\rangle \leq$		Length $[C]$		
$\sqrt{\lambda}\mathrm{Length}[C][\langle T_{tt}\rangle/c]^{1/2}$	4	Any	General	(173)
$\sqrt{\lambda}\mathrm{Length}[C]^{d-1}\langle T_{tt}\rangle+\cdots$	3,4	Small	General	(130)
$\sqrt{\lambda}\mathrm{Length}[C][\langle T_{tt}\rangle/c]^{2/3}$	3	Any	Quench+	(134)
$\partial_t \ln\langle O(x)O(0)\rangle \leq$		$\vert x\vert$		
$\Delta\sqrt{\langle T_{tt}\rangle/c}$	2	Any	General	(83)
$\Delta\vert x\vert\langle T_{tt}\rangle/c+\cdots$	2	Small	General	(92)
$\partial_x \ln\langle O(x)O(0)\rangle \leq$				
$\partial_x \ln\langle O(x)O(0)\rangle_{\mathrm{vacuum}}$	2	Any	General	(201)

VI. DISCUSSION

In this work we have proven several new upper bounds on the rate of change of entanglement entropy, spacelike Wilson loops, and equal-time two-point functions of heavy operators. The proofs apply for spatially homogeneous and isotropic states in strongly coupled CFTs with a holographic dual. We summarize our bounds in Table I. We have also provided numerical evidence that the bounds have broader validity than our proofs. We will now discuss our findings and possible future directions.

A 2d quantum weak energy condition: The bound (5) can also be seen as a quantum weak energy condition (QWEC). Let S be the entropy of be a single interval as a function of one of the endpoints p, so that $\partial_t S$ now refers to the change of S under the perturbation of this single interval endpoint, rather than both. Then we have

$$\langle T_{tt}\rangle \geq \langle T_{tt}\rangle_{\mathrm{vac}} + \frac{3}{2\pi c}(\partial_t S)^2, \tag{226}$$

while the classical weak energy condition implies that $T_{tt}\geq 0$. Equation (226) closely resembles the conformal quantum null energy condition (QNEC) [19,141–145] in two dimensions [146]. Consider $2d$ Minkowski space, where $\langle T_{tt}\rangle_{\mathrm{vac}}=0$. Letting $x^\pm$ be null coordinates, the conformal QNEC says that [141,144]

$$\langle T_{++}\rangle|_p \geq \frac{1}{2\pi}\partial_+^2 S + \frac{3}{\pi c}(\partial_+ S)^2. \tag{227}$$

The structural similarity between (226) and (227) is obvious. While (226) does not contain a second derivative, it is in principle possible that (226) could be true also for inhomogeneous states, provided we include a term $a\partial_t^2 S$ to the right hand side for some fixed constant a. In fact, the conformal QNEC suggests that $a=(4\pi)^{-1}$, since in the special case of a half-space in a homogeneous state, where $\partial_x S=0$, the conformal QNEC and $T^\mu{}_\mu=0$ implies

$$\langle T_{tt}\rangle|_p \geq \frac{1}{4\pi}\partial_t^2 S + \frac{3}{2\pi c}(\partial_t S)^2. \tag{228}$$

Strengthened bounds: Our proof that

$$\left|\frac{\mathrm{d}S_R}{\mathrm{d}t}\right| \leq \frac{1}{4}\mathrm{Area}[\partial R]c_{\mathrm{eff}}\left[\frac{16\pi}{(d-1)c_{\mathrm{eff}}}\langle T_{tt}\rangle\right]^{\frac{d-1}{d}}, \tag{229}$$

which implies that $\mathfrak{R}\leq 1$ in neutral states, only applied to thin-shell spacetimes, which are dual to CFT states where all dynamics happen at a single energy scale (that evolves with time). However, we gave numerical evidence that this bound also holds in general planar symmetric spacetimes with extended matter profiles. A natural extension of this work is trying to generalize the proof to include this. This will likely require a better understanding of nonlinearities of the Einstein constraint equations.

Next, we found that in our numerical maximization of $\mathfrak{R}$ over a ten-parameter family of initial datasets in $d = 3$, 4, that

$$\mathfrak{R} \leq v_E^{(\mathrm{SAdS})} + \delta v_E, \tag{230}$$

where

$$v_E^{(\mathrm{SAdS})} = \sqrt{\frac{d}{d-2}}\left(\frac{d-2}{2(d-1)}\right)^{\frac{d-1}{d}} \tag{231}$$

is the entanglement velocity computed in a holographic quench having a neutral final state, and δv_E a small correction that seemed to depend on the scalar potential, but which was always small for the theories we studied (less than 0.03). This hints that it might be possible to strengthen the prefactor in (229). Similarly, our numerics suggested that the prefactors of (8) could be strengthened, and furthermore that this bound is true without $\mathcal{O}(\ell^d \langle T_{tt}\rangle / c_{\mathrm{eff}})$ corrections.

$1/N$ corrections: It seems quite likely that $\mathfrak{R} \leq 1$ remains true with perturbative $1/N$ corrections. In fact, the pure QFT proofs of $\mathfrak{R} \leq 1$ for large subregions [40,42] made no assumption about large-N, so only intermediate and small subregions could be sources violation. But for small subregions we showed that $\mathfrak{R} \leq \mathcal{O}(\ell/\beta) \ll 1$ for β the effective inverse temperature, which means perturbative $1/N$ corrections are unlikely to pose a of danger [148]. For intermediate sized regions things are less clear, but for $d = 3, 4$ we numerically did not manage to push $\mathfrak{R}$ close to 1, hinting that $1/N$ corrections do not pose a danger in these dimensions.

Finite coupling: Our bounds were proven at strong coupling, but it seems possible that our bounds survive for arbitrary coupling. In [42] it was found that the entanglement velocity of a free theory (for $d > 2$) is strictly smaller than the holographic strong coupling result, suggesting that dialing up the coupling increases the capability of generating entanglement.

Primaries close to the unitarity bound: In order to turn on bulk fields dual to relevant CFT operators with scaling dimensions Δ in the window

$$\frac{d-2}{2} \leq \Delta < \frac{d}{2}, \tag{232}$$

we must consider scalars with masses

$$m_{\mathrm{BF}}^2 \leq m^2 < m_{\mathrm{BF}}^2 + 1/L^2, \tag{233}$$

and turn on the modes with slow falloffs rather than fast falloffs (see for example [149–152]). This leads to violation of the falloff assumptions (16), and causes the ordinary definition of the spacetime mass to be divergent. Then neither of the Hawking masses reduce to the CFT energy at conformal infinity. Consequently, significant modifications of our proofs would be required. The same holds if we turn on sources that perturb us away from a CFT. Things can get even more challenging, given that for some falloffs $\partial_t S$ itself might become divergent [45]. In this case we should only try to bound finite quantities, like the mutual information or the renormalized entanglement entropy [102,103], where these divergences cancel.

Bounds with charge: It is a persistent finding that $U(1)$ gauge fields tend to slow down the growth of extremal surfaces of various dimensions [33,34,43,153]. It thus seems plausible that our bounds can be strengthened by taking into account nonzero charges in the CFT. It is suggestive that, in spherical and planar symmetry, $U(1)$ gauge fields contribute energy density, but they have no pure contribution to the momentum density—that is, they only contribute to $\mathcal{J}$ through gauge covariant derivatives acting on other matter fields.

Other boundary geometries: Except for $d = 2$, our proofs always assumed the CFT lives on Minkowski space. However, our bounds survive if we compactify on a torus, so the boundary geometry is $\mathbb{R} \times T^{d-1}$, provided we make a few additional assumptions. For the bounds of the type $|\partial_t S| \leq \kappa \mathrm{Vol}[R]\langle T_{tt}\rangle + \cdots$ (and the similar bounds for Wilson loops), we should always consider regions less than half the system size—otherwise $\mathrm{Vol}[R]$ should be replaced with the volume of the complement. For bounds with multiple strips, if we have a torus, we need to make sure that the entangling surfaces are all parallel, which happens automatically in Minkowski due to the parallel postulate.

Next, our proofs for single regions should imply growth bounds for CFTs on the static cylinder $\mathbb{R} \times S^{d-1}$, as long as we take the regions to be very small compared to the curvature radius of the boundary sphere. The results for balls will translate to results for small caps, while the result for strips will translate to results for thin belts around the equator.

Why do things fall? In [53] it was proposed that the process of gravitational attraction is dual to the increase of complexity in the CFT. Assuming the complexity = volume conjecture [78], this was given a precise realization in [54–56] (see also [106]), where it was shown that the rate of change of the volume of a maximal volume slice is given by the momentum integrated on the slice. However, our formula

$$\frac{\mathrm{d}S_R}{\mathrm{d}t} = \int_X G t^a n^b \mathcal{T}_{ab} \tag{234}$$

shows that change in entanglement can also be seen as directly responsible for the radial momentum of matter. Thus, at present, “the increase of entanglement” seems like an equally good explanation for why things fall.

Relevant scalars, compact dimensions, and DEC breaking: Our proofs rely critically on the dominant energy condition—almost all steps of the proofs break without it. This rules out having scalars with negative squared mass, which are dual to relevant operators in the CFT. Nevertheless, we found numerical evidence that the bounds hold true without the DEC, as long as the scalar theories we consider allow a positive mass theorem, so that AdS is stable and $\langle T_{tt}\rangle$ is guaranteed to be positive in a uniform state.

However, there are other reasons to believe that our bounds remain true for these theories beyond our numerical findings—at least when working with top-down theories. Consider working with a theory that is a dimensional reduction and consistent truncation of type IIA, IIB, or eleven-dimensional SUGRA, so that any solution can be lifted to solutions on asymptotically $\mathrm{AdS}_{d+1}\times K$ spacetimes for some compact manifold K. These solutions will typically be warped products rather than direct products, but there exists significant evidence [154] that the entropy computed by the HRT formula in the uplifted spacetime agrees with the one computed in the dimensionally reduced spacetime—even when the product is not direct. But in the uplifted spacetime the DEC holds, since it holds for type II and eleven-dimensional SUGRA. Thus, if our methods can be generalized to work for warped compactifications over spherically symmetric AAdS_{d+1} bases, this appears to be an avenue to prove our bounds even with relevant scalars turned on. The drawback is that the proofs might have to be carried out separately for each family of compactifications.

ACKNOWLEDGMENTS

It is a pleasure to thank Sean Colin-Ellerin, Netta Engelhardt, Gary Gibbons, Matt Headrick, Hong Liu, Dan Roberts, Jon Sorce, and Brian Swingle for discussions. A. D. was supported by the University of Minnesota Doctoral Dissertation Fellowship and by the National Science Foundation Graduate Research Fellowship under Grant No. 00039202. The research of Å. F. is supported in part by the John Templeton Foundation via the Black Hole Initiative, NSF Grant No. PHY-2011905, and an Aker Scholarship. The research of Å. F. was also supported in part by the Heising-Simons Foundation, the Simons Foundation, and NSF Grant No. PHY-1748958.

APPENDIX

1. The mean curvature of X in Σ

Let now $A, B, \ldots$ be indices for tensors on X, and $\alpha, \beta, \ldots$ be indices for tensors on Σ, and consider intrinsic coordinates on Σ and X from Sec. II B. The induced metrics are

$$\begin{aligned}\mathrm{d}s^2|_\Sigma &= H_{\mu\nu}\mathrm{d}x^\mu \mathrm{d}x^\nu = B(r)\mathrm{d}r^2 + r^2[\mathrm{d}\phi^2 + \delta_{ij}\mathrm{d}x^i\mathrm{d}x^j]\\ \mathrm{d}s^2|_X &= \gamma_{AB}\mathrm{d}y^A\mathrm{d}y^B\\ &= [B(r)+r^2\Phi'(r)^2]\mathrm{d}r^2 + r^2\delta_{ij}\mathrm{d}x^i\mathrm{d}x^j. \end{aligned}\tag{A1}$$

A basis of tangent vectors to X in Σ is $\{e_A^\alpha\}$, with expressions

$$\begin{aligned} e_r^\alpha &= (\partial_r)^\alpha + \Phi'(r)(\partial_\phi)^\alpha,\\ e_i^\alpha &= (\partial_{x^i})^\alpha. \end{aligned}\tag{A2}$$

The normal to X inside Σ reads

$$n_\alpha = \sqrt{\frac{Br^2}{B+r^2(\Phi')^2}}[\Phi'(r)(\mathrm{d}r)_\alpha - (\mathrm{d}\phi)_\alpha]\tag{A3}$$

With this in hand, we can compute the mean curvature of X in Σ:

$$\begin{aligned}\mathcal{K} &= \gamma^{AB}e_A^\alpha e_B^\beta \nabla_\alpha n_\beta\\ &= \frac{1}{r\sqrt{B}[B+r^2(\Phi')^2]^{3/2}}\\ &\quad\times\left[(d-1)r^3\Phi'(r)^3 + \left(dB - \frac{1}{2}rB'\right)r\Phi' + r^2B\Phi''\right]. \end{aligned}\tag{A4}$$

2. Explicit form of $K - n^\alpha n^\beta K_{\alpha\beta}$

Noting that

$$n^\alpha = \sqrt{\frac{Br^2}{B+r^2(\Phi')^2}}\left(\frac{\Phi'(r)}{B(r)}(\partial_r)^\alpha - \frac{1}{r^2}(\partial_\phi)^\alpha\right)\tag{A5}$$

we get

$$\begin{aligned} K &= H^{\alpha\beta}K_{\alpha\beta} = \frac{1}{B}K_{rr} + \frac{d-1}{r^2}K_{\phi\phi},\\ K_{\alpha\beta}n^\alpha n^\beta &= \frac{Br^2}{B+r^2\Phi'(r)^2}\left[\frac{\Phi'(r)^2}{B^2}K_{rr} + \frac{1}{r^4}K_{\phi\phi}\right]. \end{aligned}\tag{A6}$$

Inserting $K_{rr}(r) = B(r)F(r)$ and doing some algebra, $K - n^\alpha n^\beta K_{\alpha\beta} = 0$ becomes (49).

3. Uniqueness of ODE solution

Choose units of $r_0 = L = 1$ without loss of generality, and introduce a new variable $h(r)$ through

$$\Phi'(r) = h(r)\frac{\sqrt{B(r)}}{r\sqrt{r^{2d-2}-1}},\tag{A7}$$

where we without loss of generality can take h positive. Substitute into (33), we get the ODE

$$h'(r) = (d-1)\frac{h(r)[1-h(r)^2]}{r^{2d}-r^2}, \qquad r \in (1,\infty). \tag{A8}$$

There are only two constant solutions to this equation: $h=1$ or $h=0$. $h=0$ gives the trivial solution, so $h=1$ is the only nontrivial constant solution. Now, assume instead that h is not constant, and consider two possible variable redefinitions:

$$h = \frac{e^{f_-(r)}}{\sqrt{e^{2f_-(r)}+1}}, \qquad h = \frac{e^{f_+(r)}}{\sqrt{e^{2f_+(r)}-1}}, \tag{A9}$$

The former is valid when $h<1$ while the latter when $h>1$. In terms of these variables, the ODE becomes

$$f'_\pm(r) = \frac{(d-1)r}{r^{2d}-r^2}, \tag{A10}$$

which has the unique solutions

$$f_\pm(r) = c + \frac{1}{2}\log\left(1-r^{2-2d}\right) \tag{A11}$$

for a real integration constant c. Inserting this into h gives

$$h = \frac{e^c\sqrt{r^{2d-2}-1}}{\sqrt{\pm r^{2d-2}+e^{2c}(r^{2d-2}-1)}}, \tag{A12}$$

where $\pm$ corresponds to $f_\pm$. For any real c we see that h is real valued on our domain only for the $+$ solution. But for this solution, for any real c, we see that we get

$$\lim_{r\to 1}\Phi'(r) < \infty, \tag{A13}$$

which contradicts our initial condition $\Phi'(1)=\infty$. Thus $h=1$ is the unique solution satisfying our initial condition.

4. Deriving formulas for $\partial_t S$ and $\partial_\ell S$

a. A formula for $\partial_t S$

In this section, we show that the entropy growth is proportional to the infalling matter flux. We will first need to prove that

$$\left.\frac{\mathrm{dArea}[X_t]}{\mathrm{d}t}\right|_{t=0} = \int_{\partial X} N^a \eta_a = -\frac{\mathrm{Area}[\partial R]}{L^{d-2}}\lim_{r\to\infty} r^{d-3}K_{\phi\phi} \tag{A14}$$

For the calculation, we will construct the vector η^a, which is tangent to the boundary $\partial\mathcal{M}$, and N^a, the outward unit normal to $\partial\Sigma = \partial\mathcal{M}\cap\Sigma$ in Σ, in a coordinate system. To do so, introduce the ADM coordinates adapted to the extended homology hypersurface

$$\mathrm{d}s^2|_{\mathcal{M}} = -r^2\mathrm{d}\tau^2 + H_{\mu\nu}(\tau,x)\mathrm{d}x^\nu\mathrm{d}x^\nu, \tag{A15}$$

where we took the shift to be vanishing, and the lapse to be r. $x^\mu = (r,\boldsymbol{x})$ are the coordinates on Σ, and $H_{\mu\nu}(\tau=0,x)$ its induced metric, given by (31). The extrinsic curvature of Σ reads

$$K_{\alpha\beta} = \frac{1}{2r}\partial_\tau H_{\alpha\beta}|_{\tau=0}. \tag{A16}$$

Imagine now we have the coordinates $z^i=(t,\boldsymbol{x})$ on $\partial\mathcal{M}$ and take $\partial\Sigma$ to be located at $(r=r_c, t=\tau=0)$ with a temporary cutoff $r=r_c$. We want to find embedding coordinates $(r(t),\tau(t))$ for $\partial\mathcal{M}$ such that the induced metric reads

$$\mathrm{d}s^2|_{\partial\mathcal{M}} = h_{ij}\mathrm{d}z^i\mathrm{d}z^j = \frac{r_c^2}{L^2}[-\mathrm{d}t^2 + L^2\mathrm{d}\phi^2 + L^2\mathrm{d}\boldsymbol{x}^2] \tag{A17}$$

The components of the induced metric then satisfy

$$h_{tt} = g_{rr}\dot{r}^2 - r^2\dot{\tau}^2 = -\frac{r_c^2}{L^2}, \tag{A18}$$

$$h_{\phi\phi} = g_{\phi\phi} = r_c^2. \tag{A19}$$

Taking the derivative of the second equation, and then setting $t=0$ gives a system of equations that is easily solved to give (see the Appendix of [106])

$$\dot{\tau}(0) = \left.\frac{1}{L\sqrt{1-BK_{\phi\phi}^2 r^{-2}}}\right|_{r=r_c}, \tag{A20}$$

$$\dot{r}(0) = -\left.\frac{K_{\phi\phi}}{L\sqrt{1-BK_{\phi\phi}^2 r^{-2}}}\right|_{r=r_c}, \tag{A21}$$

where we have chosen the branch $\dot{\tau}>0$. Thus, η^a in our ADM coordinate system reads

$$\eta^a = (\partial_t)^a = \dot{\tau}(0)(\partial_t)^a + \dot{r}(0)(\partial_r)^a. \tag{A22}$$

Now, the tangents to ∂X are tangent to ∂R, and the sole remaining tangent vector e_r^α in (A2) is then the normal to $\partial\Sigma$. Hence, up to a normalization C,

$$N^\mu = Ce_r^\mu = C(1,\Phi',0), \tag{A23}$$

which can be unit normalized and pushed forward to a spacetime vector yielding [in the coordinates (A15)],

$$N^a = \frac{1}{\sqrt{B(r)+r_c^2\Phi'(r)^2}}(0,1,\Phi'(r),0)|_{r=r_c}. \tag{A24}$$

We can now compute the integral on the cutoff regulated ∂X:

$$\begin{aligned}\int_{\partial X}\eta^a N_a &= -\frac{K_{\phi\phi}}{L\sqrt{1-B(r_c)K_{\phi\phi}^2/r_c^2}}\times\frac{B(r_c)}{\sqrt{B(r_c)+r_c^2(\partial_r\Phi)^2}}\\ &\quad\times r_c^{d-2}\int \mathrm{d}^{d-2}\boldsymbol{x}\\ &= -\frac{K_{\phi\phi}\sqrt{B(r_c)}}{L\sqrt{1-B(r_c)K_{\phi\phi}^2/r_c^2}}\times\sqrt{1-(r_0/r_c)^2}\\ &\quad\times r_c^{d-2}\frac{\mathrm{Area}[\partial R]}{L^{d-2}},\end{aligned}\tag{A25}$$

where we have used the differential equation for the embedding function $\Phi(r)$. In the large r limit, the asymptotic behaviors are

$$B(r)\sim\mathcal{O}(r^{-2}),\qquad K_{\phi\phi}\sim\mathcal{O}(r^{-(d-3)}).\tag{A26}$$

Taking the cutoff to the boundary, one finds the area growth to be given by (38).

b. A covariant formula for $\partial_t S$

Now let us write the integral formula for $\partial_t S$ in a covariant way. Letting t^a be the future unit normal to Σ and n^a the outward normal to X tangent to Σ, we have for some function G on X that only depends on r:

$$\begin{aligned}&8\pi G_N\int_X G(r)t^a n^b\mathcal{T}_{ab}\\ &=\int \mathrm{d}^{d-2}\boldsymbol{x}\int_{r_0}^{\infty}\mathrm{d}r r^{d-2}\sqrt{B+r^2(\Phi')^2}G(r)n^r\mathcal{J}\\ &=\frac{\mathrm{Area}[\partial R]}{L^{d-2}}\int \mathrm{d}r\frac{r_0^{d-1}}{r^d}G(r)\mathcal{J}\sqrt{r^{2d-2}-r_0^{2d-2}},\end{aligned}\tag{A27}$$

where we used (35) and (A3). Letting

$$G(r)=\frac{2\pi r^d}{(d-1)r_0^{d-1}},\tag{A28}$$

we get a covariant formula for the entropy growth

$$\frac{\mathrm{d}S_R}{\mathrm{d}t}=\int_X G t^a n^b\mathcal{T}_{ab}.\tag{A29}$$

c. A formula for $\partial_\ell S$

Consider a one-parameter family of HRT surfaces X_ℓ anchored at the strip region region R_ℓ, given by (18), but letting now ℓ vary, holding t fixed. Taking the vector field η^a generating the flow of ∂X_ℓ to be $\eta^a|_{\partial\mathcal{M}}=\frac{1}{L}(\partial_\phi)^a$, (36) becomes

$$\frac{\mathrm{d}}{\mathrm{d}\ell}\mathrm{Area}[X_\ell]=\frac{\mathrm{Area}[\partial R]}{L^{d-1}}\lim_{r\to\infty}r^{d-2}g_{\phi\phi}N^\phi.\tag{A30}$$

Using (35), (A15), and (A24), this evaluates to

$$\begin{aligned}\frac{\mathrm{d}}{\mathrm{d}\ell}\mathrm{Area}[X_\ell]&=\frac{\mathrm{Area}[\partial R]}{L^{d-1}}\lim_{r\to\infty}r^d\frac{\Phi'}{\sqrt{B+r^2(\Phi')^2}}\\ &=\frac{\mathrm{Area}[\partial R]}{L^{d-1}}r_0^{d-1}.\end{aligned}\tag{A31}$$

5. Computing $\partial_t\|X_t\|$

The derivation of (150) is almost identical to the derivation in Appendix A 4. Let us just highlight what must be changed. First, we do not have an explicit formula for $\Phi'(r)$, but this does not matter, since everything we need is its rate of falloff, which we can read off to be $\Phi'(r)\sim\mathcal{O}(1/r^{q+2})$ from (145). Next, in (A25), it is sufficient to replace $r_c^{d-2}\to r_c^q$. After doing that, and taking into account that $K_{\phi\phi}$ now has falloff $\mathcal{O}(1/r^{q-1})$, the $r_c\to\infty$ limit of (A25) with these modifications gives (150).

6. Geometric properties of X and Σ

Let us now prove various properties of extended homology hypersurfaces. We give the proof for HRT surfaces of strips and comment how the proofs are modified for $(q+1)$-dimension extremal surfaces anchored at spheres.

Lemma 7. The extended homology hypersurface Σ of a strip region in a spacetime with planar symmetry cannot have a throat in its interior, i.e., a radius where $B(r)$ diverges.

Proof. Assume for contradiction that Σ has a throat T in its interior—if there are multiple, take T to be the outermost one. Since Σ by definition terminates at the plane tangent to the tip of X, this means that X must pass beyond the throat. But if X crosses the throat, there must be a point on $X\cap T$ where X is not tangent to T. Let now $U\subset\Sigma$ be the region outside T, which we can always cover with a coordinate system

$$\begin{aligned}&\mathrm{d}s^2|_U=B(r)\mathrm{d}r^2+r^2\mathrm{d}\boldsymbol{x}^2,\qquad r\in[r_T,\infty),\\ &B(r_T)=\infty,\qquad B(r>r_T)<\infty.\end{aligned}\tag{A32}$$

where the throat is at $r=r_T$. The fact that X is not tangent to T means that $|\Phi'(r_T)|<\infty$. But the solution for the extremal surface reads

$$\Phi'(r)^2=\frac{B(r)}{r^2(r^{2d-2}c-1)}\tag{A33}$$

for some constant c, and so $|\Phi'(r_T)|=\infty$, which is a contradiction. Hence T cannot exist in the interior of Σ. ■

This proof goes through the case of X anchored at a dimension q sphere, as discussed in Sec. III, simply taking Φ' to be computed from (145).

Next, we have the following:

Lemma 8. The HRT surface X of a strip region R can only have one turning point.

Proof. Assume for contradiction that X has multiple turning points. Then there must be at least one turning point of X in the interior of Σ that is a local maximum of the embedding function $r(\phi)$. Let $\phi = \phi_t$ where this turning point occurs, and let us restrict our attention to a neighborhood $\phi \in \mathcal{O}_\epsilon = (\phi_t, \phi_t + \epsilon)$, where we can invert $r(\phi)$ to get $\Phi(r)$, describing the embedding in $\mathcal{O}_\epsilon$. We see that $\Phi'(r) < 0$ and $\Phi''(r) < 0$ in this neighborhood. Now, the equation for the HRT surface in the neighborhood $\mathcal{O}_\epsilon$ is

$$(d-1)r^3\Phi'^3 + r^2 B\Phi'' + r\Phi'\left(dB - \frac{r}{2}B'\right) = 0. \tag{A34}$$

Since we are in the interior of Σ, B is bounded on $\mathcal{O}_\epsilon$ by Lemma 7. Since Φ' diverges at the turning point, the equation for Φ' near the turning point reads

$$r^2 B\Phi'' = -(d-1)r^3\Phi'^3\left[1 + \mathcal{O}\left(\frac{1}{(\Phi')^2}\right)\right], \tag{A35}$$

where the correction can be neglected to arbitrarily good precision since B is bounded. But this implies that Φ'' and Φ' must have opposite signs in $\mathcal{O}_\epsilon$ for sufficiently small ϵ, which is a contradiction. Hence X can only have one turning point. ■

We did not consider the case where $r'(\phi_t) = r''(\phi_t) = 0$, but this was shown to be ruled out by [123]. Also, note that this proof survives the case of spherical boundary anchoring and a $(q+1)$-dimensional extremal surface, since the new term $(\Phi')^3\chi(r)$ in the extremality Eq. (141) is subleading at the prospective turning point, since it scales like $\chi \sim 1/\Phi'$. Thus, (A35) remains true [up to a numerical factor and an $\mathcal{O}(1/\Phi')$ correction].

7. General extremality conditions

Let

$$H_{ab} = g_{ab} + t_a t_b \tag{A36}$$

be the induced metric on Σ. Then we have $h^{ab} = H^{ab} - \delta^{IJ} n_I^a n_J^b$, and so

$$\begin{aligned}\mathcal{K}^0 &= (H^{ab} - \delta^{IJ} n_I^a n_J^b)\nabla_a t_b \\ &= K - \delta^{IJ} n_I^a n_J^b \nabla_{(a} t_{b)} \\ &= K - \delta^{IJ} n_I^a n_J^b K_{ab},\end{aligned} \tag{A37}$$

where we in the last line used that $n_I^a n_J^b$ is tangent to Σ, which projects out the difference $\nabla_{(a} t_{b)} - K_{ab}$. Now, a collection of tangents e_I^α to X are

$$\begin{aligned}e^\alpha{}_r &= (\partial_r)^\alpha + \Phi'(r)(\partial_\phi)^\alpha \\ e^\alpha{}_i &= (\partial_{\Omega^i})^\alpha,\end{aligned} \tag{A38}$$

where i runs over sphere directions. The unit normals to X (in Σ) are

$$\begin{aligned}n^r{}_\alpha &= \alpha(\mathrm{d}r)_\alpha + \beta(\mathrm{d}\phi)_\beta, \\ n^j{}_\alpha &= r(\mathrm{d}z^j)_\alpha,\end{aligned} \tag{A39}$$

for some α, β we now work out, and where the coordinates are with respect to the index μ on Σ. r, j should be view as indices in the orthonormal tangent basis labeled by I on X. Now

$$\begin{aligned}0 &= n^r{}_\alpha e^\alpha{}_r = \alpha + \beta\Phi'(r), \\ 1 &= H^{\alpha\beta} n^r{}_\alpha n^r{}_\beta = \frac{\alpha^2}{B} + \frac{\beta^2}{r^2}.\end{aligned} \tag{A40}$$

Solving for α, β, we get

$$n^r{}_\alpha = \sqrt{\frac{Br^2}{B + r^2(\Phi')^2}}(\Phi'(\mathrm{d}r)_\alpha - (\mathrm{d}\phi)_\alpha), \tag{A41}$$

Now we want to impose

$$\mathcal{K}^0 = K - \delta^{IJ} n_I^a n_J^b K_{ab} = 0. \tag{A42}$$

Explicitly we have

$$\begin{aligned}K &= \frac{1}{B}K_{rr} + \frac{1}{r^2}K_{\phi\phi} + \frac{w^{ij}}{r^2\phi^2} \times \underbrace{\phi^2 w_{ij} K_{\phi\phi}}_{K_{ij}} + \frac{d-2-q}{r^2}\underbrace{K_{\phi\phi}}_{K_{zz}}, \\ &= \frac{1}{B}K_{rr} + \frac{d-1}{r^2}K_{\phi\phi},\end{aligned} \tag{A43}$$

and

$$\delta^{IJ} n_I^a n_J^b K_{ab} = (n^{rr})^2 K_{rr} + (n^{r\phi})^2 K_{\phi\phi} + (d-2-q)\frac{1}{r^2}K_{\phi\phi}. \tag{A44}$$

Thus, with $K_{rr} = BF$, condition (A42) reads

$$[1 - B(n_r^r)^2]F + \left[\frac{q+1}{r^2} - (n_r^\phi)^2\right]K_{\phi\phi} = 0 \tag{A45}$$

Using the explicit formula for n_r^r, n_r^ϕ in (A41), inserting the explicit formula for $\Phi(r)$ from (145), and solving for $F(r)$, we find (153).

Note also that thanks to (A43) and (75) is unchanged, and so the proof that $\pm\theta_\pm[\partial\Sigma] \geq 0$ for strips survive for dimension–$q+1$ surfaces anchored at q-spheres.

[1] A. Kitaev and J. Preskill, Phys. Rev. Lett. **96**, 110404 (2006).
[2] M. Levin and X.-G. Wen, Phys. Rev. Lett. **96**, 110405 (2006).
[3] A. Hamma, R. Ionicioiu, and P. Zanardi, Phys. Lett. A **337**, 22 (2005).
[4] C. H. Bennett and S. J. Wiesner, Phys. Rev. Lett. **69**, 2881 (1992).
[5] C. H. Bennett, G. Brassard, C. Crépeau, R. Jozsa, A. Peres, and W. K. Wootters, Phys. Rev. Lett. **70**, 1895 (1993).
[6] C. H. Bennett and G. Brassard, Theor. Comput. Sci. **560**, 7 (2014).
[7] L. Bombelli, R. K. Koul, J. Lee, and R. D. Sorkin, Phys. Rev. D **34**, 373 (1986).
[8] J. D. Bekenstein, Phys. Rev. D **9**, 3292 (1974).
[9] D. N. Page, Phys. Rev. Lett. **71**, 3743 (1993).
[10] S. Ryu and T. Takayanagi, Phys. Rev. Lett. **96**, 181602 (2006).
[11] V. E. Hubeny, M. Rangamani, and T. Takayanagi, J. High Energy Phys. 07 (2007) 062.
[12] M. Van Raamsdonk, Gen. Relativ. Gravit. **42**, 2323 (2010).
[13] A. C. Wall, Phys. Rev. D **85**, 104049 (2012); **87**, 069904 (E) (2013).
[14] A. C. Wall, Classical Quantum Gravity **31**, 225007 (2014).
[15] A. Almheiri, D. Marolf, J. Polchinski, and J. Sully, J. High Energy Phys. 02 (2013) 062.
[16] J. Maldacena and L. Susskind, Fortschr. Phys. **61**, 781 (2013).
[17] T. Faulkner, A. Lewkowycz, and J. Maldacena, J. High Energy Phys. 11 (2013) 074.
[18] N. Engelhardt and A. C. Wall, J. High Energy Phys. 01 (2015) 073.
[19] R. Bousso, Z. Fisher, S. Leichenauer, and A. C. Wall, Phys. Rev. D **93**, 064044 (2016).
[20] A. Almheiri, N. Engelhardt, D. Marolf, and H. Maxfield, J. High Energy Phys. 12 (2019) 063.
[21] G. Penington, J. High Energy Phys. 09 (2020) 002.
[22] H. Casini and M. Huerta, Phys. Lett. B **600**, 142 (2004).
[23] P. Calabrese and J. L. Cardy, J. Stat. Mech. (2005) P04010.
[24] H. Casini and M. Huerta, J. Phys. A **40**, 7031 (2007).
[25] I. R. Klebanov, D. Kutasov, and A. Murugan, Nucl. Phys. **B796**, 274 (2008).
[26] P. V. Buividovich and M. I. Polikarpov, Nucl. Phys. **B802**, 458 (2008).
[27] R. C. Myers and A. Sinha, Phys. Rev. D **82**, 046006 (2010).
[28] R. C. Myers and A. Sinha, J. High Energy Phys. 01 (2011) 125.
[29] H. Casini and M. Huerta, Phys. Rev. D **85**, 125016 (2012).
[30] S. N. Solodukhin, arXiv:1304.4411.
[31] V. Balasubramanian, A. Bernamonti, J. de Boer, N. Copland, B. Craps, E. Keski-Vakkuri, B. Muller, A. Schafer, M. Shigemori, and W. Staessens, Phys. Rev. Lett. **106**, 191601 (2011).
[32] V. Balasubramanian, A. Bernamonti, J. de Boer, N. Copland, B. Craps, E. Keski-Vakkuri, B. Muller, A. Schafer, M. Shigemori, and W. Staessens, Phys. Rev. D **84**, 026010 (2011).
[33] H. Liu and S. J. Suh, Phys. Rev. Lett. **112**, 011601 (2014).
[34] H. Liu and S. J. Suh, Phys. Rev. D **89**, 066012 (2014).
[35] M. Mezei and D. Stanford, J. High Energy Phys. 05 (2017) 065.
[36] C. Jonay, D. A. Huse, and A. Nahum, arXiv:1803.00089.
[37] M. Mezei, Phys. Rev. D **98**, 106025 (2018).
[38] K. Van Acoleyen, M. Mariën, and F. Verstraete, Phys. Rev. Lett. **111**, 170501 (2013).
[39] S. Bravyi, Phys. Rev. A **76**, 052319 (2007).
[40] T. Hartman and N. Afkhami-Jeddi, arXiv:1512.02695.
[41] A proof was also given in [42] for half-planes, taking linear growth of entanglement as an assumption. For quenches, it was proven for large regions holographically in [43], together with many other properties of quenches.
[42] H. Casini, H. Liu, and M. Mezei, J. High Energy Phys. 07 (2016) 077.
[43] M. Mezei, J. High Energy Phys. 05 (2017) 064.
[44] In fact, since generic QFTs can have state-dependent divergences in S_R [45], $\partial_t S_R$ can be divergent in some theories, and so (4) cannot be true in all relativistic QFTs. This means that a generalization of the proofs of [40,42] to include contributions not scaling with volume is impossible without more input on the theories under consideration.
[45] D. Marolf and A. C. Wall, J. High Energy Phys. 10 (2016) 109.
[46] For holographic CFTs, (5) also improves on a bound proven for single intervals of any size in all $2d$ CFTs by [40], which can be written as $\mathfrak{R} \leq \coth\left(\pi\ell\sqrt{\frac{\pi c}{6\langle T_{tt}\rangle}}\right)$.
[47] P. Calabrese and J. L. Cardy, Phys. Rev. Lett. **96**, 136801 (2006).
[48] P. Calabrese and J. Cardy, J. Stat. Mech. (2007) P06008.
[49] See [50] for a discussion of a different definition of $\mathfrak{R}$, where $s_{\rm th}$ is replaced by the vacuum-subtracted entanglement entropy per volume in the final state. With this definition, $\mathfrak{R}$ is $O(1)$ for small subregions, but it can exceed 1.
[50] S. Kundu and J. F. Pedraza, Phys. Rev. D **95**, 086008 (2017).
[51] N. Bao, A. Chatwin-Davies, B. E. Niehoff, and M. Usatyuk, Phys. Rev. D **101**, 066011 (2020).
[52] S. Ryu and T. Takayanagi, J. High Energy Phys. 08 (2006) 045.
[53] L. Susskind, arXiv:1802.01198.

[54] J. L. F. Barbón, J. Martín-García, and M. Sasieta, J. High Energy Phys. 07 (2020) 169.
[55] J. L. F. Barbon, J. Martin-Garcia, and M. Sasieta, Phys. Rev. D **102**, 101901 (2020).
[56] J. L. F. Barbon, J. Martin-Garcia, and M. Sasieta, J. High Energy Phys. 04 (2021) 250.
[57] Allowing two-sided spacetimes means that automatically allow mixed states on a single CFT, since we can always find a purification dual to a wormhole, simply by gluing a second CPT-conjugate copy of the spacetime to itself along the HRT surface [58].
[58] N. Engelhardt and A. C. Wall, J. High Energy Phys. 05 (2019) 160.
[59] V. Balasubramanian and P. Kraus, Commun. Math. Phys. **208**, 413 (1999).
[60] In this case, depending on how slow the falloffs are, subleading divergences in the entropy might become state dependent [45], in which case $\mathfrak{R} \leq 1$ cannot remain true. See discussion in Sec. VI.
[61] J. Abajo-Arrastia, J. Aparicio, and E. Lopez, J. High Energy Phys. 11 (2010) 149.
[62] W. Baron, D. Galante, and M. Schvellinger, J. High Energy Phys. 03 (2013) 070.
[63] E. Caceres and A. Kundu, J. High Energy Phys. 09 (2012) 055.
[64] D. Galante and M. Schvellinger, J. High Energy Phys. 07 (2012) 096.
[65] S. H. Shenker and D. Stanford, J. High Energy Phys. 03 (2014) 067.
[66] S. H. Shenker and D. Stanford, J. High Energy Phys. 12 (2014) 046.
[67] Y.-Z. Li, S.-F. Wu, Y.-Q. Wang, and G.-H. Yang, J. High Energy Phys. 09 (2013) 057.
[68] I. Aref'eva, A. Bagrov, and A. S. Koshelev, J. High Energy Phys. 07 (2013) 170.
[69] P. Caputa, G. Mandal, and R. Sinha, J. High Energy Phys. 11 (2013) 052.
[70] T. Ugajin, arXiv:1311.2562.
[71] C. T. Asplund and A. Bernamonti, Phys. Rev. D **89**, 066015 (2014).
[72] M. Alishahiha, M. R. Mohammadi Mozaffar, and M. R. Tanhayi, J. High Energy Phys. 09 (2015) 165.
[73] P. Fonda, L. Franti, V. Keränen, E. Keski-Vakkuri, L. Thorlacius, and E. Tonni, J. High Energy Phys. 08 (2014) 051.
[74] V. Keranen, H. Nishimura, S. Stricker, O. Taanila, and A. Vuorinen, Phys. Rev. D **90**, 064033 (2014).
[75] M. Alishahiha, A. Faraji Astaneh, and M. R. Mohammadi Mozaffar, Phys. Rev. D **90**, 046004 (2014).
[76] E. Caceres, A. Kundu, J. F. Pedraza, and D.-L. Yang, J. High Energy Phys. 06 (2015) 111.
[77] A. Buchel, R. C. Myers, and A. van Niekerk, J. High Energy Phys. 02 (2015) 017; 07 (2015) 137(E).
[78] D. Stanford and L. Susskind, Phys. Rev. D **90**, 126007 (2014).
[79] K. Babaei Velni, M. R. Mohammadi Mozaffar, and M. H. Vahidinia, J. High Energy Phys. 08 (2020) 129.
[80] S. Leichenauer and M. Moosa, Phys. Rev. D **92**, 126004 (2015).
[81] C. Ecker, D. Grumiller, and S. A. Stricker, J. High Energy Phys. 07 (2015) 146.
[82] V. Ziogas, J. High Energy Phys. 09 (2015) 114.
[83] K. A. Sohrabi, Phys. Rev. D **96**, 026012 (2017).
[84] E. Caceres, M. Sanchez, and J. Virrueta, J. High Energy Phys. 09 (2017) 127.
[85] M. Rangamani, M. Rozali, and A. Vincart-Emard, J. High Energy Phys. 04 (2016) 069.
[86] D. Roychowdhury, Phys. Rev. D **93**, 106008 (2016).
[87] C. Ecker, D. Grumiller, P. Stanzer, S. A. Stricker, and W. van der Schee, J. High Energy Phys. 11 (2016) 054.
[88] A. O'Bannon, J. Probst, R. Rodgers, and C. F. Uhlemann, Phys. Rev. D **96**, 066028 (2017).
[89] S. F. Lokhande, G. W. J. Oling, and J. F. Pedraza, J. High Energy Phys. 10 (2017) 104.
[90] R. C. Myers, M. Rozali, and B. Way, J. Phys. A **50**, 494002 (2017).
[91] I. Y. Aref'eva, M. A. Khramtsov, and M. D. Tikhanovskaya, J. High Energy Phys. 09 (2017) 115.
[92] V. Jahnke, J. High Energy Phys. 01 (2018) 102.
[93] M. Flory, J. Erdmenger, D. Fernandez, E. Megias, A.-K. Straub, and P. Witkowski, J. Phys. Conf. Ser. **942**, 012010 (2017).
[94] D. Ávila, V. Jahnke, and L. Patiño, J. High Energy Phys. 09 (2018) 131.
[95] H. Ghaffarnejad, E. Yaraie, and M. Farsam, Gen. Relativ. Gravit. **51**, 10 (2019).
[96] W. Fischler, V. Jahnke, and J. F. Pedraza, J. High Energy Phys. 11 (2018) 072; 02 (2021) 149(E).
[97] J. Kudler-Flam, I. MacCormack, and S. Ryu, J. Phys. A **52**, 325401 (2019).
[98] J. Couch, S. Eccles, P. Nguyen, B. Swingle, and S. Xu, Phys. Rev. B **102**, 045114 (2020).
[99] Y. Ling, Y. Liu, and Z.-Y. Xian, Chin. Phys. C **44**, 023101 (2020).
[100] M. Mezei and W. van der Schee, Phys. Rev. Lett. **124**, 201601 (2020).
[101] K. Goto, M. Nozaki, K. Tamaoka, M. T. Tan, and S. Ryu, arXiv:2112.14388.
[102] H. Liu and M. Mezei, J. High Energy Phys. 04 (2013) 162.
[103] H. Liu and M. Mezei, J. High Energy Phys. 01 (2014) 098.
[104] N. Bao, C. Cao, S. Fischetti, and C. Keeler, Classical Quantum Gravity **36**, 185002 (2019).
[105] $\hat{\Sigma}$ and Σ are unique. Planar symmetry means that $(\mathcal{M}, g_{ab})$ can be foliated by planes, and every point $p \in X$ lies in some plane in this foliation. Demanding planar symmetry of Σ requires that the full leaf intersected by p is included in Σ, and so we have a one-parameter family of codimension–2 surfaces picked out by X, which thus fully specifies Σ, and similarly for $\hat{\Sigma}$.
[106] N. Engelhardt and Å. Folkestad, J. High Energy Phys. 01 (2022) 040.
[107] S. Fischetti and T. Wiseman, Classical Quantum Gravity **34**, 125005 (2017).
[108] C. Fefferman and C. R. Graham, *Elie Cartan et les Mathématiques d'aujourdhui (Astérisque)* (1985), p. 95, http://www.numdam.org/item/AST_1985__S131__95_0/.
[109] C. Graham and J. M. Lee, Adv. Math. **87**, 186 (1991).
[110] C. R. Graham and E. Witten, Nucl. Phys. **B546**, 52 (1999).

[111] For $d = 3$ it is also known as the Geroch-Hawking mass [112–115], and its was used to prove the Riemannian Penrose inequality [115].
[112] R. Geroch, Ann. N.Y. Acad. Sci. **224**, 108 (1973).
[113] P. Jang and R. Wald, J. Math. Phys. (N.Y.) **18**, 41 (1977).
[114] X. Wang, J. Diff. Geom. **57**, 273 (2001).
[115] G. Huisken and T. Ilmanen, J. Diff. Geom. **59**, 353 (2001).
[116] We have here taken the outward and inward null vectors, k_+^a and k_-^a, respectively, to be $k_\pm^a = 2^{-1/2}(t^a \pm n^a)$.
[117] For thin-shell spacetimes $\mathcal{J}(\rho)$ can be a delta function, but we can safely assume this delta function does not have support exactly at $r = r_0$.
[118] S. W. Hawking, J. Math. Phys. (N.Y.) **9**, 598 (1968).
[119] Å. Folkestad, Phys. Rev. Lett. **130**, 121501 (2023).
[120] S. A. Hayward, Phys. Rev. D **53**, 1938 (1996).
[121] This monotonicity is a planar-symmetric Lorentzian version of the monotonicity the Riemannian Hawking mass under inverse mean curvature flow, which has been used to prove Riemannian Penrose inequalities [112–115]. A Lorentzian flow with a monotonic Lorentzian Hawking mass for compact surfaces in three dimensions, without any symmetry assumptions, was studied in [122].
[122] H. Bray, S. Hayward, M. Mars, and W. Simon, Commun. Math. Phys. **272**, 119 (2007).
[123] N. Engelhardt and S. Fischetti, Classical Quantum Gravity **32**, 195021 (2015).
[124] R. Bousso, J. High Energy Phys. 06 (1999) 028.
[125] J. D. Brown and M. Henneaux, Commun. Math. Phys. **104**, 207 (1986).
[126] The normalization here is such that a planar black brane would have the metric $-f\mathrm{d}t^2 + f^{-1}\mathrm{d}r^2 + r^2\mathrm{d}\boldsymbol{x}^2$ with $f = r^2/L^2 - \mu(\infty)r^{2-d}$.
[127] By the same kind of analysis as in Appendix A 6, we cannot have additional turning points where $\Phi'(r)$ diverges, and so we have strict inequality in the lower bound.
[128] J. M. Maldacena, Phys. Rev. Lett. **80**, 4859 (1998).
[129] S.-J. Rey and J.-T. Yee, Eur. Phys. J. C **22**, 379 (2001).
[130] N. Engelhardt and Å. Folkestad, J. High Energy Phys. 07 (2022) 031.
[131] T. Hertog, G. T. Horowitz, and K. Maeda, J. High Energy Phys. 05 (2003) 060.
[132] W. Boucher, Nucl. Phys. **B242**, 282 (1984).
[133] P. Townsend, Phys. Lett. **148B**, 55 (1984).
[134] If we choose completely arbitrary bulk scalar theories, we have no positive mass theorem, so we can have $\langle T_{tt}\rangle < 0$ in a homogeneous state, and the bounds are clearly violated. But in these situations there is no sensible holographic dual.
[135] M. Cvetic, M. J. Duff, P. Hoxha, J. T. Liu, H. Lu, J. X. Lu, R. Martinez-Acosta, C. N. Pope, H. Sati, and T. A. Tran, Nucl. Phys. **B558**, 96 (1999).
[136] H. Lu and C. N. Pope, Phys. Lett. B **467**, 67 (1999).
[137] H. Lu, C. N. Pope, and T. A. Tran, Phys. Lett. B **475**, 261 (2000).
[138] M. Cvetic, H. Lu, and C. N. Pope, Phys. Rev. Lett. **83**, 5226 (1999).
[139] P. Breitenlohner and D. Z. Freedman, Phys. Lett. **115B**, 197 (1982).
[140] P. Breitenlohner and D. Z. Freedman, Ann. Phys. (N.Y.) **144**, 249 (1982).
[141] A. C. Wall, Phys. Rev. D **85**, 024015 (2012).
[142] R. Bousso, Z. Fisher, J. Koeller, S. Leichenauer, and A. C. Wall, Phys. Rev. D **93**, 024017 (2016).
[143] C. Akers, J. Koeller, S. Leichenauer, and A. Levine, arXiv:1610.08968.
[144] J. Koeller and S. Leichenauer, Phys. Rev. D **94**, 024026 (2016).
[145] S. Balakrishnan, T. Faulkner, Z. U. Khandker, and H. Wang, J. High Energy Phys. 09 (2019) 020.
[146] See [147] for a study on how the QNEC constrains entanglement growth.
[147] M. Mezei and J. Virrueta, arXiv:1909.00919.
[148] The discovery of quantum extremal surfaces (QES) [18] far from classical extremal surfaces [20,21] might make this argument somewhat less convincing, but it seems unlikely that these dominate/exist for small subregions, whose QES reside close to the conformal boundary.
[149] T. Hertog and G. T. Horowitz, J. High Energy Phys. 07 (2004) 073.
[150] M. Henneaux, C. Martinez, R. Troncoso, and J. Zanelli, Phys. Rev. D **70**, 044034 (2004).
[151] M. Henneaux, C. Martinez, R. Troncoso, and J. Zanelli, Ann. Phys. (Amsterdam) **322**, 824 (2007).
[152] T. Hertog and K. Maeda, J. High Energy Phys. 07 (2004) 051.
[153] D. Carmi, S. Chapman, H. Marrochio, R. C. Myers, and S. Sugishita, J. High Energy Phys. 11 (2017) 188.
[154] P. A. R. Jones and M. Taylor, J. High Energy Phys. 08 (2016) 158.